ÉCOLE POLYTECHNIQUE
FÉDÉRALE DE LAUSANNE

eawag
aquatic research

Gravity-driven membrane filtration with hollow-fiber membranes operated in inside-out mode: distribution and characteristics of the biofilm inside and outside the fiber and feed-strategy effects on the performance

Master Thesis

Environmental Engineering
École polytechnique fédérale de Lausanne (EPFL)

Wei Yin

Supervision

Prof. Dr. Urs von Gunten (EPFL)
Dr. Céline Jacquin (Eawag)

August 26, 2022

Abstract

This research focus on the biofilm development in the lumen of inside-out hollow fiber (HF) gravity driven membrane (GDM), as well as the influence of feed and maintenance strategies to improve the permeability of HF membrane. Moreover, the influence of quality of water for backwash is also investigated, to see how it changes the permeate quality. To be specific, this research addresses the three aspects: (1) the biofilm development within time in the lumen of inside out HF membrane, (2) the influence of feed strategy (namely top feed and top_bottom feed) and backwash frequency (backwash on daily bases and threshold) on the permeability of HF membrane, as well as the biofilm development in the lumen, (3) the influence of quality of backwash water (with/without assimilable organic carbon and disinfectant) on the permeate quality. To be noticed that, in the (2) aspect, in order to further understand the behavior of modules with different feed strategies and backwash frequencies in real operation, high turbidity events were simulated to see their resilience during and after the extreme situations. To this end, modules with inside-out operation mode 7-capillaries hollow fiber membranes with different operational times and strategies were evaluated. The flux as well as the permeate quality were measured. Some of the modules were sacrificed to investigate their inside biofilm. The first result shows that inside the lumen of inside-out HF membrane, biofilm were not homogeneously distributed, while the feeding end had more biofilm accumulated and the other end had less, and this phenomenon becomes more apparent on membrane with longer operational time. The following result is that feeding from both ends increased the flux and homogenize the inside biofilm distribution; threshold backwash provided high flux rate but less permeate due to the high consumption of permeate for backwash; threshold backwash modules recovered sooner than daily backwash modules, but both of them recovered after several backwash sequences. The last finding is that the cells in the water for backwash contributed to the cells in the permeate, as well as the biofilm on the membrane; regardless of the quality of water for backwash, there were always cells appeared in the permeate. In conclusion, biofilm in the lumen of the inside-out HF membrane is developing within time and its distribution is influenced by the feed strategy; top_bottom feed provided relatively homogeneous biofilm distribution as well as resistance and higher flux, comparing to top feed; threshold backwash provided less net permeate but showed stronger resilience during high turbidity event compared to daily backwash; quality of water for backwash influenced the permeate quality, and it was hard to prevent cells regrowth in the permeate regardless of the quality of water for backwash.

Keywords: Gravity-driven membrane (GDM), inside-out HF membrane, biofilm gradient, feed strategy, regrowth in permeate

Table of Contents

List of Abbreviations

AOC	Assimilable organic carbon
ATP	Adenosine triphosphate
BW	Backwash
GDM	Gravity-driven membrane
HF	Hollow fiber
HRT	Hydraulic retention time
TCC	Total cell count
LM	Light microscopy
OCT	Optical coherence tomography
PBS	Phosphate-buffered saline solution
TMP	Transmembrane pressure
TOC	Total organic carbon

List of Figures

List of Tables

Chapter 1

Introduction

Membrane filtration is a pressure-driven separation method that can be used to mechanically sieve particles, microorganisms molecules and ions (24). Ultrafiltration is a membrane process, with the nominal membrane pore size of 0.001–0.05 μm and driving force of 2–5 bar (23). It is wildly used in water purification area. There is a demand that UF membrane operation should maintain its strength and safety and reduce the cost (2), while energy consumption contributes a large part of UF operation (10). Gravity driven membrane (GDM) filtration is an ultrafiltration process but with a lower pressure (0.04 - 0.1 bar), which produces less permeate (2–10 L/m^2/h) (3; 19). It becomes appealing as it has lower energy consumption than a normal ultrafiltration membrane bio-reactor (10) and now it is implemented for drinking water treatment (21; 18). Some GDM platforms do not apply chemical cleaning, which leads to the growth of biofilm on the surface of the membrane (19). In order to reduce the price of GMD operation, reducing its occupied space is one option. It has been approved that comparing to flat sheet membrane, outside-in hollow fiber (HF) membranes have a lower footprint and cost associated with GDM filtration (16). It is also possible to achieve GDM filtration with in-side out HF membrane, but due to its limited space for biofilm growth, its flux, 3.9 $\pm$ 1.2 L/m^2/h, is relatively lower (25) comparing to a outside-in HF membrane, with a flux of 8.0 $\pm$ 0.8 L/m^2/h after 52 days of operation. Membrane fouling is always one main reason for low flux and biopolymers, colloidal humic acids and other microorganism are considered to be the cause of fouling and flux drop for flat sheet membranes (18). Research has demonstrated that biofilm dominates the resistance for filtration (9) and with different operation methods, there is a gradient of biofilm on the surface of flat sheet membranes (5). Due to its special configuration of inside-out HF membranes, the fouling process is hard to be observed. Normally the biofilm is observed with in situ optical methods, which is difficult to apply to inside-out HF membranes. By cutting the fiber longitudinally and with the help of light microscopy, Boller (4) pointed out that there is a gradient of biofilm in the capillaries of inside-out HF membrane when it was fed from one end, in which the top part (the end water goes in) accumulated more biofilm than the other end. Her research showed that this gradient, especially the top part, contributed to the high resistance of the whole fiber (4). However, the HF membrane used in her study was sacrificed and studied after 596 days of operation. Whether this gradient had already shown at an early stage and how it developed remains uncertain.

Since the low flux is still a drawback of inside-out HF membranes, increasing the flux is one critical point to study. Feed strategies and backwash frequency are two aspects studied in this research. Some drinking water treatment plants have applied feeding from two ends of of the HF membrane (15; 21); some studies proved that different shear strength impacts the resistance of the membrane (25; 9). The feeding from both ends, rather than one end of the HF membrane may help to

increase its flux. Study from Boller (4) shows that there was a different biofilm gradient in the capillaries of HF membrane fed from both ends, and this strategy led to less flux drop and helped the permeability to remain at a high level, which is 28.2 ± 7.1% higher comparing to feeding from one end (4). However, how does the flux trend correlate to the resistance and biofilm gradient does not explicit in her study. Apart from the feed strategies, backwash is also considered to be a good way to remove the biofilm and increase the flux. A study shows that backwash eases the fouling of ceramic membrane bioreactor (26). Boller also (4) pointed out that threshold backwash (backwash when the flux drops to a certain level) helps to maintain the flux at a significant higher level (21% higher) comparing to daily backwash, but with the drawback of using too much permeate for backwash, leading to a lower net water production (4.4% lower than the one of daily backwash) (4). As a conlimialion of previous research on the gradient of the inside bioflim, it is interesting to explain this phenomenon, to find out whether the high gross production but low net production is correlated to the biofilm property.

Feed strategy and backwash frequency are two measurement to maintain the flux of a membrane. In the reality, these measurements should also be working during extreme events, like high turbidity influent, which may bring particles to the membrane and largely reduce its flux. Peter-Varbanets et al.(17) stated that influent turbidity around 30 NTU does not show a significant impact on flux in a long term; Boller (4) also observed that after the backwash, flux can be recovered even it was decreased by a high turbidity event with maximum 90 NTU for 6 hours. However, the particle size of the influent was not well controlled during both studies (the previous one used wastewater and latter one used river water). One could imagine that within the same turbidity, particles with different sizes would cause different levels of flux drop and whether they could be recovered by backwash.

Apart from flux, permeate quality is another important factor to assess GDM filtration performance. Research from Nicolas Derlon et al. (7) shows that biofilm on the filtration side (the side of the dirty water) of membranes affect the permeate quality regarding AOC concentration (decrease in short term, increase in long term). Boller (4) stated that soon after a backwash, there was a leap of total cell count (TCC) and assimilable organic carbon (AOC) in the permeate. By linking these two studies, one could come up with the hypothesis that it is the biofilm on the permeate side (the side clean water goes out) that influences the permeate quality in terms of TCC. The research from Boller also showed that after several HRT (3 and 6), the TCC in the permeate went back to the level of the permeate before backwash (4), and this may indicate that the TCC in the permeate is associated with the backwash. But it is unclear how the biofilm is introduced to the outside of the membrane and how it is associated with the permeate quality.

The scopes of this research are: (1) to investigate the biofilm gradient and development within time inside the HF membrane and its link to flux dynamics; (2) to study the influence of different feed strategies, backwash frequency as well as high turbidity on the biofilm distribution inside the HF membrane; and (3) find out how the quality of water for backwash influence the HF membrane permeate quality in terms of TCC and cell regrowth. To this end, inside-out 0.9 mm Multibore® 7-capillaries HF membrane modules in GMD operation with different operation time (20 days, 60 days, 180 days and 670 days), strategies (top and top_bottom) and backwash frequency (daily and threshold) were carried out in one platform. Each module was sacrificed at a certain time and the HF membranes were taken out to study their inside biofilm gradient; To study the influence of high turbidity with different particle size, a high turbidity simulation was carried out, the flux before and after the event was compared. Finally, in order to study the relationship between the quality of water for backwash and the quality of permeate, permeate, NaOCl solution, PBS solution and acetate in PBS solution was prepared for backwash of four different modules, and their permeate was collected to analysis the TCC and its regrowth, respectively.

Chapter 2

Material and methods

2.1 Membrane

A membrane module includes 8 to 10 HF membranes (membrane surface is 0.20 m^2 or 0.22 m^2 accordingly) runing in parallel. The HF membrane is a 0.9 mm Multibore® from Inge Dupont. 0.9 mm 8-capillaries HF membranes with pores that are 20 nm and are composed of modified polyethersulfone (PES) were used. The module shell is transparent polyvinyl chloride (PVC) (12). 6 valves control one module's feed and backwash, a bucket together with a scale measure the real-time weight of permeate. The weight data is stored in the data base (DataPool) every 30 seconds, so that the flux can be calculated afterwards with the following equation:

$$J = \frac{\Delta V}{A \times \Delta t} \tag{1}$$

where J is the permeate flux [$L/m^2/h$], A is the membrane surface area [m^2], and ΔV is the permeate volume [L] collected during the time step Δt [h].

There is also a temperature sensor in the feed water canal to provide real time temperature data to help to normalize the flux at 20 ° with equation 2:

$$J_{20} = J_T \times \left(1.784 - (0.0575 \times T) + (0.0011 \times T^2) - (10^{-5} \times T^3)\right) \tag{2}$$

where J_{20} is the normalized flux at 20°C [$L/m^2/h$], J_T is the permeate flux at temperature T [$L/m^2/h$], and T is the temperature in the raw water canal [°C].

To eliminate short-term changes, the permeate flux was computed continuously over a time step of 5 minutes. Permeate flux values were only recorded when filtering occurred (not during drainage, backwash, relaxation and forward flush). Additionally, the total amount of generated water for each module is measured.

Prior to use, each module was conditioned by running through a deionized water filtering step for at least 30 minutes at a transmembrane pressure (TMP) from 0.3 to 0.05 bar. Then, TMPs of 0.09, 0.25, and 0.30 bar were applied to assess each module's permeability. The flux was measured at each pressure, and the flux as a function of TMP was plotted. The slope of the generated curve was then used to determine the permeability.

To solve the 3 questions proposed in Chapter. 1, there are 3 groups of modules that are operated

within different method. Figure. 2.1 shows the general characteristics of the modules in each groups.

Table 2.1: Characteristics of Multibore® membrane modules used in the present study

	Modules group 1	**Modules group 2**	**Modules group 3**
Operational days [days] *	20, 60 and 670**	180	21
Membrane surface area [m^2]	0.22	0.20	0.20
Backwash frequency	daily, weekly and none**	daily and threshold**	daily
Feed type	top feed	top feed and top-bottom feed**	top feed
Backwash water quality	permeate	permeate	permeate, PBS, acetate and NaOCl**
Abbreviation	dBW_20, dBW_60, dBW_670, wBW_20, wBW_60, wBW_670, nBW_20, nBW_60, nBW_670**	dBW_top, dBW_top_bottom, tBW_top, tBW_top_bottom**	dBW_permeate, dBW_PBS, dBW_acetate, dBW_NaOCl**

* Number of operational days before the modules were sacrificed (cut to investigate its inside); dBW, wBW and nBW are abbreviation of daily bachwash, weekly backwash and no backwash

** More than one condition for one module group means that there are more than 1 module are operated within this group and each of them are operated differently

_20, _60 and _670 refer to number of operational days before the modules were sacrificed (cut to investigate its inside); dBW, wBW, nBW and tBW are abbreviation of daily backwash, weekly backwash, no backwash and threshold backwash; _top and _top_bottom mean the place where the modules were fed; _permeate, _PBS, _acetate and _NaOCl refer the quality of the water for backwash.

2.2 GDM platform set up

A platform in the Aquatikum at Eawag was built to hold all the experimental facilities for this research. This platform is able to hold up to 30 modules at the same time. Chriesbach river (Dübendorf, Switzerland) provides river water resource for all the modules' influent. The influent went through a coarse filter (300 μm) and pumped up to a cylindrical sedimentation tank (155 L, HRT = 100 min), after which the influent is stored in a feed tank (240 L), feeding water equally to all the membrane systems (TMP = 80 mbar). The permeate of membrane system is collected and stored in a permeate tank (80 L), which is 2.8 meters higher than the backwash inlet of module, and the backwash tank provides gravity driven backwash for all modules at TMP = 280 mbar. The sedimentation tank and feed tank are cleaned on a weekly basis. This is to reduce the amount of accumulated particles which may block the modules at top and significantly reduce the flux. Fig. 2.1 illustrate the general figure of the platform.

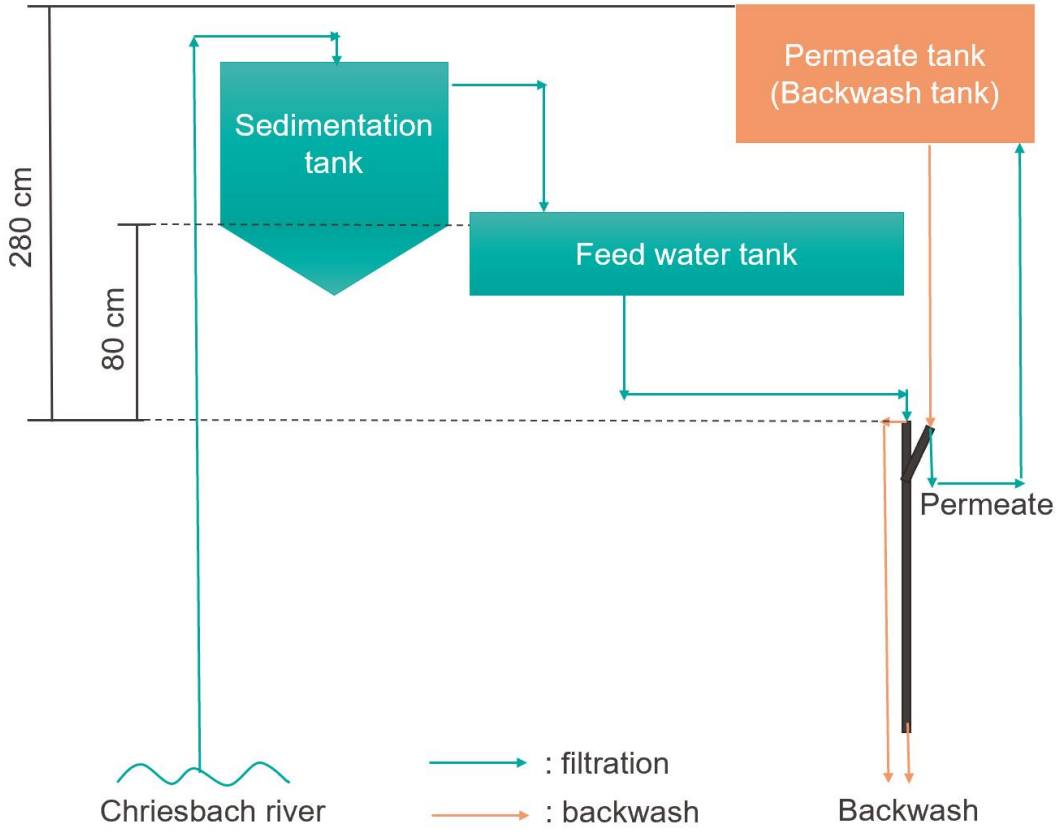

Figure 2.1: The GDM platform. Only one module is shown on this figre, while it's possible to accommodate 30 modules

2.2.1 Module operation

Fig. 2.2 shows the top feed module (on the left) and top_bottom feed module (on the right). Valve 1, 2 and 3 were remotely controlled; a, b, c, d, e and f are the inlets/outlets of water flow. During filtration, water (river water in this research) goes from valve 1 a (and valve 2 f for top_bottom feed) and goes out through valve 3 d; during backwash, the water for backwash firstly goes though valve 3 c and goes out of the module at valve 1 b and 2 e. Every week, the backwash flux was manually measured. The backwash water of each backwash cycle was collected and weighed individually. The backwash flux was also calculated using equations 1 and 2. Backwash flux helps to calculated the permeate production ratio. Especially for modules group 1 and 2, all the modules are backwashed with the permeate collected in the backwash tank. The proportion of the backwash permeate to the total amount of permeate could be helpful to determine the best backwash frequency. Equation 3 shows this calculation:

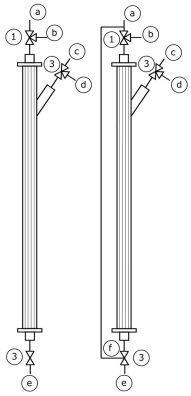

Figure 2.2: Modules with top feed and top bottom feed

$$E = \frac{W_{permeate} - W_{backwash}}{W_{permeate}} \tag{3}$$

where E is the backwash efficiency, $W_{permeate}$ is the weight of permeate in a certain time (e.g.: 1 week), and $W_{backwash}$ is the wight of the amount of permeate used for backwash during this time.

2.3 Resistance measurements

After operating the different modules for the desired period mentioned in Table. 2.1, modules were stopped and sacrificed so that the fibers inside can be taken out for the measurement of resistance (Section. 2.3) and physical and chemical analysis of the biofilm (Section. 2.5).

Modules were cut from both extremity together with the ends of the fibres. In total, 3 fibers from each cut module were selected randomly. For each of the 3 fibers, it was cut into 3 equal-length part which are named top, middle and bottom sequentially depending on its position on the original module.

To measure the resistance each collected fiber or fiber section, the bottom end was blocked with a valve and the top end was connected to a rotor pump, which continuously pumped water into the fiber. A pressure sensor was placed between the rotor pump and fiber to fix a transmembrane pressure of 100 mbar for the resistance measurement. The pressure was changed by changing the rotation speed of rotor pump. Once the transmembrane pressure was stable, the produced permeate was collected for 1 minute and the maximum and minimum pressure within this time was monitored. The collected permeate was weighed to calculate the resistance using the following equation:

$$R = \frac{TMP}{J_{20} \times \mu_{20}} \tag{4}$$

where R is the resistance [m^{-1}], TMP is the transmembrane pressure [bar], J_{20} is the normalized flux at 20°C [$m^3/m^2/h$] and μ_{20} is the dynamic water viscosity at 20°C [bar h]

The protocol for resistance measurement is as follows:

Step 1) Rinse the top of the module in order to remove any solids that have accumulated, measuring the flux of the whole module; (R_t)

Step 2) Cut the shell of the module and take fibers out; cut the fibers in 3 sections with equal length of 45 cm (or 43 cm), namely top, middle and bottom part;

Step 3) Measure the resistance of each section
- (i) measure the resistance directly
- (ii) clean the outside part of the fiber with a clean sponge to remove the outside biofilm ($R_{p\text{-biofilm}}$)
- (iii) apply a backwash (TMP = 0.9 bar) to remove the inside biofilm ($R_{bw\text{-}r}$)
- (iv) perform a chemical cleaning with 200 mg/L NaOCl at pH 12 for 24 hours (immerse the fiber in the NaOCl solution) ($R_{cc\text{-}r}$ and R_{ir})

The total resistance of a considered fiber section (R) can be calculated using the resistance in series model:

$$R = R_m + R_t + R_{p\text{-biofilm}} + R_{bw\text{-}r} + R_{cc\text{-}r} + R_{ir} \tag{5}$$

where R_m is the clean membrane resistance deduced from the initial permeability [m^{-1}] as described in 2.2; $R_{cc\text{-}r}$ is the resistance reduced by chemical cleaning; R_{ir} is the resistance after the fiber was chemically cleaned.

Biofilm samples were collected during steps 3.ii), 3.iii) and 3.iv) for further analyses of TOC, particle size distribution and ATP.

Table 2.2 summarizes the resistances used in the present study and their abbreviations.

Table 2.2: Summary of different resistances and their abbreviations

Resistance abbreviation	**Resistance definition**
R_t	Resistance associated to the solids accumulating at the top part of the module
R_m	Clean membrane resistance
$R_{p\text{-}biofilm}$	Resistance associated with the biofilm developing outside the fiber
$R_{bw\text{-}r}$	Resistance associated with the particles and biofilm inside the fiber that can be removed by backwash and flush
$R_{cc\text{-}r}$	Resistance associated with the particles and biofilm inside the fiber that cannot be removed by backwash or flush, but chemical cleaning
R_{ir}	Resistance due to pore blocking, internal fouling, or membrane ageing, which cannot be removed by chemical cleaning

2.4 Particle size disribution

2.4.1 Particle size distribution measurement

Static light scattering (SLS), also called Laser Diffraction, was performed with an LS 13 320 Particle Size Analyzer from Beckman and Coulter. The instrument measured in the range between 1 to 2000 μm.

Particle size distribution measurement was carried out for the backwash water from modules in module group 1, specifically dBW_20, dBW_60, dBW_670, wBW_20, wBW_60, wBW_670, nBW_20, nBW_60, nBW_670. Moreover, this is also carried out for the backwash water from each part of the cut modules mentioned in 2.3. The particle size distribution measurement of cut fiber carries out after the resistance test and the following backwash.

2.4.2 Simulation of high turbidity events

Goransson (11) reported that during precipitation, river turbidity may exceed 50 NTU and up to 90 NTU. During dry seasons, turbidity falls to 10 NTU. Based on these parameters, high turbidity events were carried out to investigate how influent particles influence HF membranes. Two types of feed waters were used to simulate high turbidity events: (1) Chriesbach water with accumulated particle of two weeks (the sedimentation tank wasn't cleaned for two weeks) (2) Bentonite solution (ben). In both cases, the influent turbidity was fixed between 60 and 80 NTU and the feed water tank was manually stirred every 20 minutes to resuspend the particles. Each time the influent was

stirred, the influent was sampled for turbidity measurement. The experiment was stopped when the turbidity fell below 10 NTU, the experiment ended.

The effect of simulated high turbidity events on module group 2 was explored by (1) comparing flux values before, during and after the turbidity event (2) measuring the backwash frequency of threshold backwashed modules during the event.

Analyses of backwash particles determined the fate of particles entering membranes. Before and after the turbidity event, the TSS of the backwash was measured. For threshold backwashed modules, TSS from the first backwash after the turbidity event was investigated. TSS in input water was quantified and compared to TSS removed by backwash during the turbidity events. The method for TSS measurement is provided in Section. 2.4.2 is t.

Total suspended solids (TSS) measurements

Total suspended solids (TSS) in backwash water measures solids and biofilm detachment throughout the course of each backwash cycle and for each backwash line. TSS was measured by passing the collected backwash water through a 90 mm, 0.45 μm-pore filter paper. Before filtering, the filter paper was washed with deionized water, dried overnight at 105°C, then cooled for 5 minutes in a desiccator. Prior to filtration, the filter paper was weighed using an accurate scale. After filtering the sample, the filter paper was rebaked overnight under 105°C, cooled for five minutes, and then weighed. The calculation for TSS amount and concentration is given below:

$$TSS\ [mg] = W_1 - W_2 \tag{6}$$

$$TSS\ [mg/L] = \frac{W_1 - W_2}{V_{sample}} \tag{7}$$

where W_1 is the weight of filter + dried residue [mg], W_2 is the weight of filter [mg], and V_{sample} is the sample solution volume [L].

2.5 Biofilm imaging

Topographical analysis is carried out for modules from group 1 and 2, providing images to illustrate the biofilm distribution inside the HF membrane to explain the development of biofilm within time and different feed strategies.

Optical coherence tomography (OCT))

By longitudinally cutting of the module, the inner surface, together with the biofilm was exposed. Optical coherence tomography (OCT, model 930nm Spectral Domain, Thorlabs GmbH, Dachau, Germany) show the section view of the fiber surface, and the thickness and roughness can be computed according to the image.

Light microscopy (LM)

With the sample from OCT, Light microscopy (VHX-7000 Series Digital Microscope from KEYENCE) was used to take a close picture of the fiber and with its associate software, it provided the coverage ratio of the membrane. The coverage ratio is calculated with the biofilm-covered area divided by the total area of the HF membrane. A camera with high resolution of color distinguishes a

manually set color range, and automatically calculates the area with the same color captured by its lens.

2.6 Biofilm chemical composition analysis

The nature, composition, and behavior of the biofilm might be deduced from its biological characterization. With this study, one may identify whether the biofilm is composed of dormant particles or living cells, as well as whether or not there are variations across fiber sections. To determine the amount and kind of biofilm, measurements of TOC, ATP were performed. The ratios of ATP to TOC were used to assess the relative activity of both the detached biofilm and the cells.

2.6.1 Total organic carbon (TOC)

Total organic carbon (TOC) measures the total concentration of organic compounds in water (6). It comprises live bacterial cells, dead cells, breakdown products, and other organic components. In this study, a TOC analyzer (TOC-L, Shimadzu) was used. Samples were homogenized before measuring. TOC was measured for all the backwash and permeate samples in module group 1 and 2, as well as the backwash water from cut fibers.

2.6.2 Adenosine triphosphate (ATP)

To assess the activity of live cells in the biofilm, ATP measurements were performed. ATP was measured with luminescence assays, with the reagent for BacTiter-Glo® Microbial Cell Viability Assay from Promega, ATP was measure. One could determine the activity of the targeted solution by:

$$A = \frac{ATP(mol/L/m^2)}{TOC(mol/L/m^2)} \tag{8}$$

where A is the factor that determine the activity of the solution. One solution can have

2.6.3 FCM measurement

Using a flow cytometer (CytoFLEX from Beckman and Coulter), the total cell counts are measured. The microbial cells in the studied samples were stained with 10 µL of SYBR® green I or SYBR® green I/PI per mL of sample in an Eppendorf tube for TCC or ICC, respectively. After 5 seconds of vortexing, the Eppendorfs were incubated in the dark at 37°C for 12 to 15 minutes. The samples that had been stained and incubated were then transferred to a 96-well plate by adding 200 µL each well. Each sample was measured twice. Washing wells with 200 µL of nanopure water were set up in duplicate between each sample to reduce the likelihood of cross-contamination. The flow cytometers enable the detection and counting of cells as they travel through a laser light beam. The laser excites the SYBR® green-labeled fluorescent cell components, causing light scattering and fluorescence emission that may be measured by different detectors. Depending on the fluorescent dye employed, it is possible to determine the number of total cells per µL.

For the purpose of determining how a biofilm influences the cells that are already present in the permeate, the TCC was measured for module group 1 and 2. To determine whether the backwash

provides cells in the permeate, and how the permeate quality changes within different kinds of backwash water, the TCC was measured for module group 3.

2.6.4 Regrowth potential

The concentration of bacteria that can be sustained by nutrients such as nitrogen and phosphorus in the water is what is measured by the regrowth potential (28). Regrowth analyses were performed on the samples described in section 2.6.3. The regrowth potential in the permeate was evaluated by making a comparison between the TCC 3 days after the first sample (day 0). For a period of three days, the samples that were collected in the carbon-free glass vials of 40 mL were kept at room temperature and all samples were subjected to the identical conditions. A growth factor was used to quantify the regrowth potential, and it was computed as follows:

$$Regrowth\ potential = \frac{TCC_{day3}}{TCC_{day0}} \tag{9}$$

Regrowth potential was measured for module group 3, which sheds light on the quality of the permeate in different backwash quality conditions. As shown in Table. 2.1, modules in group 3 is backwashed with permeate, PBS (8 g/L NaCl, 0.2 g/L KCl, 1.6 g/L $Na_2HPO_4{\cdot}2H_2O$ and 0.2 g/L KH_2PO_4), acetate (200 μg_C/L) in PBS solution and 200 mg/L NaOCl solution. Permeate and acetate both provide food to possible bacteria in the water and on the membrane, PBS provides nothing but a stable environment, while NaOCl disinfects the membrane surface. Modules backwashed with PBS, acetate solution and NaOCl were equipped with separate backwash tanks. The operation mode is the same as the modules described in 2.2.1.

2.7 Statistical analysis

In previous sections, it was described that many methods were used to identify biofilm and its behavior, the correlation between then becomes critical to provide a comprehensive analysis. Multi-correlation (linear regression) was used to assess the correlation between all of the data.

Chapter 3

Results and discussion

3.1 Link between the flux and the Biofilm distribution along the fiber

3.1.1 Effect of the backwash frequency on the link between flux and biofilm distribution along the fiber

Biofilm inhomogeneous distribution is considered to be one visible phenomenon of flux difference between modules with different backwash frequency (3; 5; 4). Thus understanding the flux difference and finding a representative flux value is the first step to interpret the biofilm distribution difference. Flux is destabilized by biofilm, but up until now, there is no study focusing on biofilm distribution inside the inside-out HF membrane. Therefore, the dBW, wBW and nBW modules operating 20 days were studied and their fluxes as a function of the operational time are shown in Fig. 3.1:

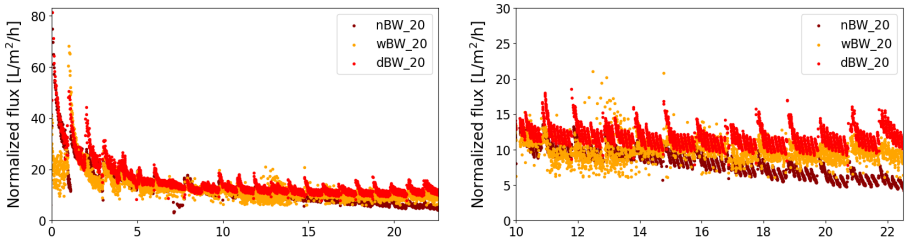

Figure 3.1: Flux of nBW, wBW and dBW modules at the first 20 days of the operation

Fig. 3.1 shows the flux of nBW_20, wBW_20 and dBW_20 modules in their 20 first days of operation. The flux of all modules had the same sharp decrease in the first 8 days of operation. Afterwards, the flux stabilized. This trend is similar to the one generaly observed for GDM systems (25). The difference in backwash frequency revealed different effect on the flux, especially after day 15 there was a clear flux difference between the nBW_20 module and the module maintained with backwash.

After 8 days of operation, the flux of dBW module became relatively stable at 13.8 $\pm$ 5.2 L/m^2/h. Compared to another study, for which the dBW module's flux stayed at 11 $\pm$ 0.4 L/m^2/h (25),

our observed data was at a comparable range. The flux drop is 0.05 L/m^2/h/d (calculated with the average flux of day 8 and day 20), which is lower than 0.36 L/m^2/h/d, the flux drop of dBW in the study by Boller (4).

The flux of wBW modules reached its stable period at day 12, with a flux of 11.2 ± 4.1 L/m^2/h and flux drop from day 12 to 20 was 0.08 L/m^2/h/d (calculated with the average flux of day 12 and day 20), which is similar to 0.07 L/m^2/h/d, the flux drop of wBW in the study by Boller (4). Compared to the dBW and the wBW modules, nBW module did not really reach its stable period from day 15 to 20, the difference in flux comparing to dBW became more and more obvious. The flux drop is 0.8 L/m^2/h/d from day 8 to 12. Therefore, the flux at day 20 could be a representative value of nBW, it is 5.3 L/m^2/h.

Different flux value of the dBW, wBW and nBW modules indicate that each module may have different biofilm properties. Therefore, all modules were sacrificed for further experiment.

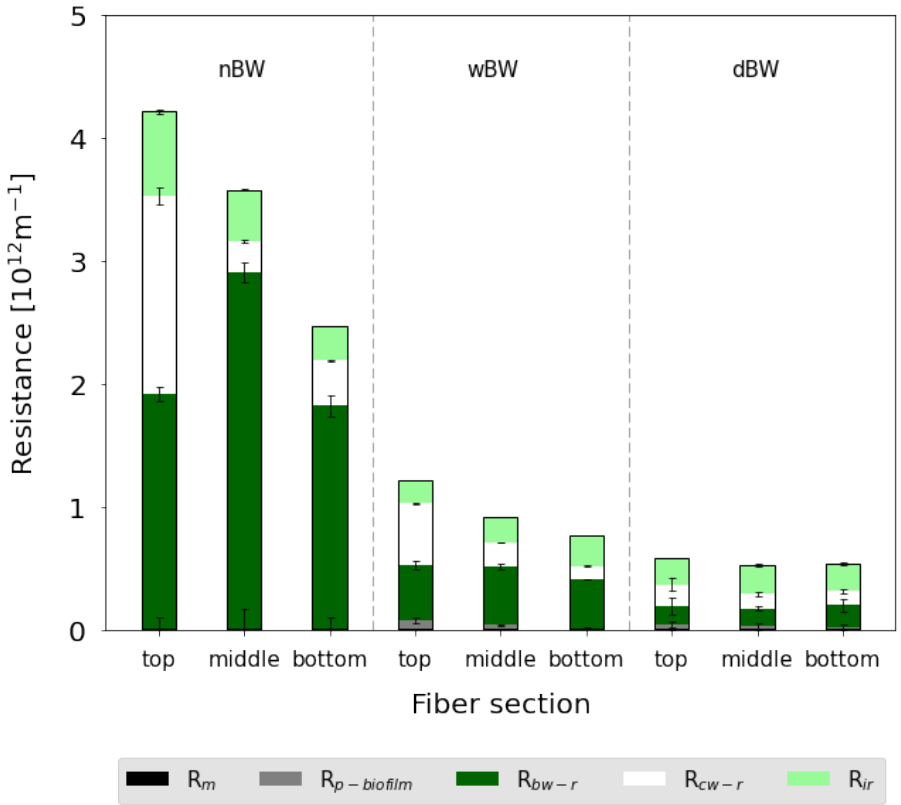

Figure 3.2: Resistance of nBW, wBW and dBW modules operating for 20 days. Resistance is measured with the method described in section 2.3

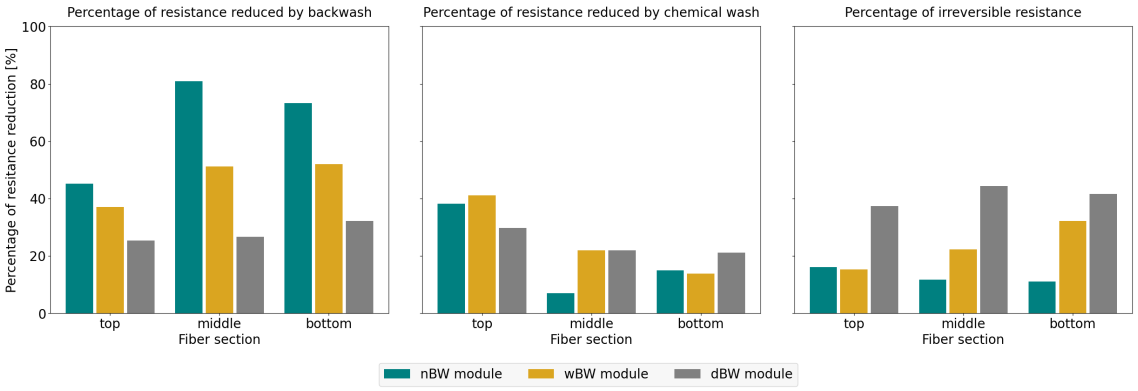

Figure 3.3: Percentage of resistance reduced by backwash and chemical cleaning. Resistance is measured with method mentioned in subsection 2.3

The resistance results shown in Fig. 3.2 confirm the difference in flux trend linked to the backwash frequency observed in Fig. 3.1. Fig. 3.2 shows that the resistance of a new membrane is negligible compared to resistance from other sources. Especially in the top part of the nBW module, 20 days of operation had largely increased its resistance to approximately $4\times10^{12}\mathrm{m}^{-1}$, which is about 4 times of that of wBW module and 6 times of dBW module. In addition to the highest resistance, nBW membrane also shows an obvious resistance decrease from top to bottom, with a resistance of about $2.5\times10^{12}\mathrm{m}^{-1}$. The wBW module also shows a similar trend but not as obvious as the one from the nBW module, while the dBW module does not have this trend and its resistance is similar among all 3 sections of it. Therefore, it seems that the backwash was working better in the middle and bottom sections of the fiber rather than the top section, for wBW and nBW modules. As shown in Fig. 3.3, for wBW and nBW modules, resistance reduced by backwash in the top part is always lower than that in middle and bottom part. Especially to the nBW module, the resistance decreased by backwash at top is about 45% of its total resitance, while in the middle section, it is 82%. Chemical cleaning helps to remove all the biofilm attached to the fiber, and the resistance measured after it has no contribution from biofilm. In contrary to backwash, the resistance reduction contributed by chemical cleaning is more obvious in the top part regardless of the maintenance. This trend is also clearer for the nBW module, for which the resistance reduced by chemical cleaning was approximately 40%, 4 times than that of the middle section. A similar trend was observed in a previous study that backwash was not efficient to the top part of the module, while chemical cleaning was, and an opposite trend was observed in the other parts of the fiber (4). These results indicate that the top section, which is the inlet of the influent is sensitive to chemical cleaning, but shows stronger resistance to backwash regardless of the kinds of maintenance. With more frequent backwash, each part of the fiber becomes more homogeneously sensitive during backwash and chemical cleaning. Moreover the irreversible resistance increased with the frequency of backwash. This means that if one module is backwashed from its very beginning of operation, it will remain easy to be backwashed and chemically cleaned within 20 days. If a module is less frequently backwashed, or even not backwashed, it will be hard to reduce its resistance after 20 days operation only by backwash. However, with the help of chemical cleaning, the modules with more backwashes showed more irreversible resistance after chemically cleaned, while the modules with less backwashes had less. According to the research on GDM in rain water treatment (27), backwash is helping to ease the flux drop at the beginning, but may lead to a worse stablized flux after long term operation. Our result by now is comparable to this research at the beginning stage. But whether this trend could be observed after a long term operation cannot be answered, and

this will be discussed in section. 3.1.2

Since chemical cleaning is targeted to the biofilm and it helped the fiber to reduce the resistance apparently, the amount of biofilm and the resistance of the fiber may be correlated in some way, and this will be discussed with Fig. 3.4

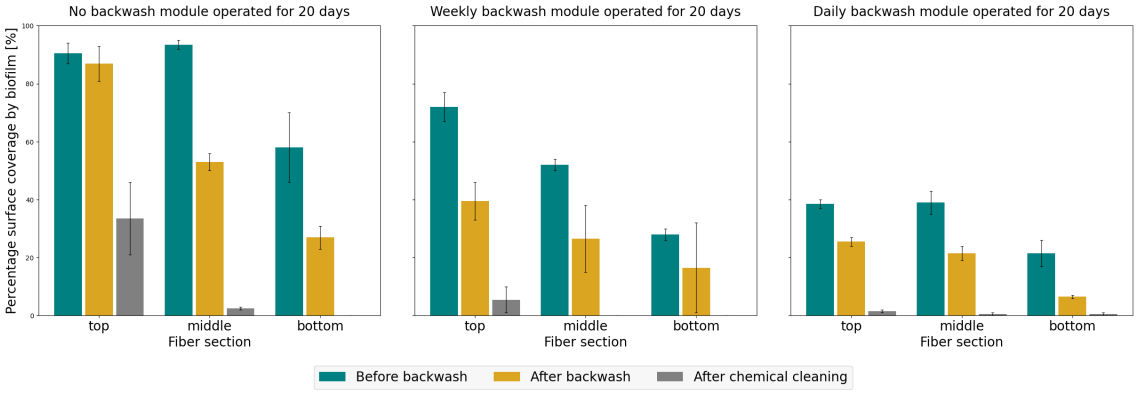

Figure 3.4: Coverage ratio by inside biofilm of dBW, wBW and nBW module operating for 20 days. Coverage ratio is measured with method described in section 2.5

With 20 days of operation, the dBW, the wBW and the nBW modules have shown dissimilarity; the more frequent the backwash, the less the inner surface is covered by biofilm. Irrespective the modules, the coverage percentage of top section was higher than the other sections. Moreover, the coverage ratio of all sections decrease largely after chemical cleaning. This proves that the biofilm deposited into the fibers is sensitive to the chemical cleaning and it could contribute to resistance reduction. As we observed here that the feed end has more biofilm accumulation, while the other end does not, the feeding strategy may also influence the coverage ratio as well as the resistance. This will be further discussed in section. 3.2.

3.1.2 Effect of the operation time on the link between flux and biofilm distribution along the fiber

Section. 3.1.1 shows the biofilm gradient as a result of different maintenance. According to the first 20 days of operation, dBW module's resistance, as well as coverage ratio of inside surface from different parts of the fiber, is relatively homogeneous, while the other modules, namely nBW and wBW module started to show a gradient. All these results indicate that the dBW module is the most interesting and with highest potential module if one would like to have a long term perspective of a GDM since the others has shown the trend at an early stage. From another aspect, the dBW module has the highest flux, this also indicates that there is larger chance the module will be running for a long time. There is also study shows that stratification may appear to modules feed with river water (8). However, the question remains: What is the temporal dynamic development of the biofilm along the fiber when modules are backwashed on a daily basis?

Fig. 3.5 is an extension of Fig. A.1 (in the Appendix A), showing the flux trend of the dBW module until 670 days of operation. After a sharp drop, flux reached 13.8 ± 5.2 L/m^2/h after 8 days of operation (this has been described in section. 3.1.1). After 60 days, the flux dropped to 9.2 ± 0.9 L/m^2/h (value calculated between day 50 and 60). There is still a gap between these two values, from 13.8 to 9.2, after operating 40 days, and a similar phenomenon was observed in a previous study (25), in which a flux drop after it was stable appeared at day 51.

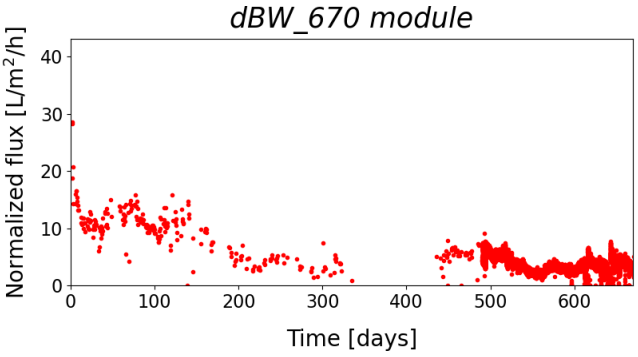

Figure 3.5: Evolution of the flux dBW module for 670 days of operation

However, there was a big flux fluctuation at day 43, and up until 180 days, more fluctuations happened. The average flux is calculated with its last five days' value, which is 4.5 ± 1.1 L/m^2/h. As to the flux of modules operating for 670 days, there are more fluctuation after 500 days, so it is hard to come up with a representative flux value and flux drop for long term operation. If calculated with the the last 10 days' data (day 660 to day 670), the average flux value of dBW is 3.2 L/m^2/h ± 2.7 L/m^2/h.

similar to what was observed in section. 3.1.1, there is flux difference between modules with different operation modes. Thus it is interesting to study the inside biofilm property of modules with different feed strategies and backwash frequencies.

Fig. 3.6 shows that dBW module had a similar trend as nBW and wBW (shown in Fig. 3.2), that its top section had more resistance than the others, and there is a clear increase of resistance with time, from 5.88 × 10^{11} /m at day 20 to 3.64 × 10^{12} at day 670. Moreover, the resistance among different sections of one fiber was changing from homogeneous at 20 days to contrasting at 670 days.

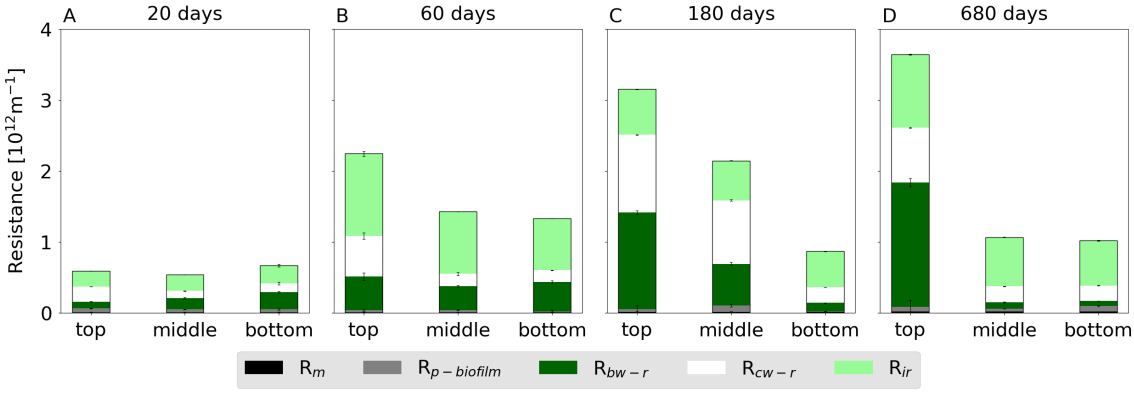

Figure 3.6: Resistance of dBW operated for different times. Fig A, B, C and D are the resistance of modules sacrificed after 20, 60, 180 and 670 days of operation respectively. Resistance is measured with the method described in section 2.3

Fig. 3.7 shows the multicorrelation between all the data included in section. 3.1.2. "Coverage" refers to coverage ratio described in section. 2.5; "ATP/TOC_BW", "ATP_BW" and "particle size_BW" means the ATP concentration, ATP/TOC concentration and particle size distribution in the backwash water, which described in the protocol step 3). (iii) in section. 2.3 and section. 2.4; "ATP/TOC_total" and "ATP_total" are the scratched biofilm from fiber directly. In the Fig. 3.7, the darkest red indicates that there is a perfect positive correlation between two variable while the darkest blue means there is a perfect negative correlation. Grey means no correlation. It seems that coverage ratio and ATP_total have good correlation with the resistance mentioned shown in Fig. 3.6, so the coverage ratio and ATP data are analyzed.

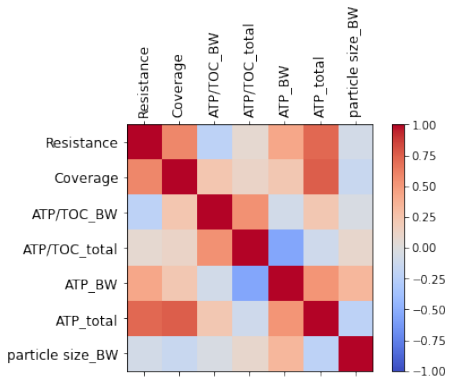

Figure 3.7: Multicorrelation of different data

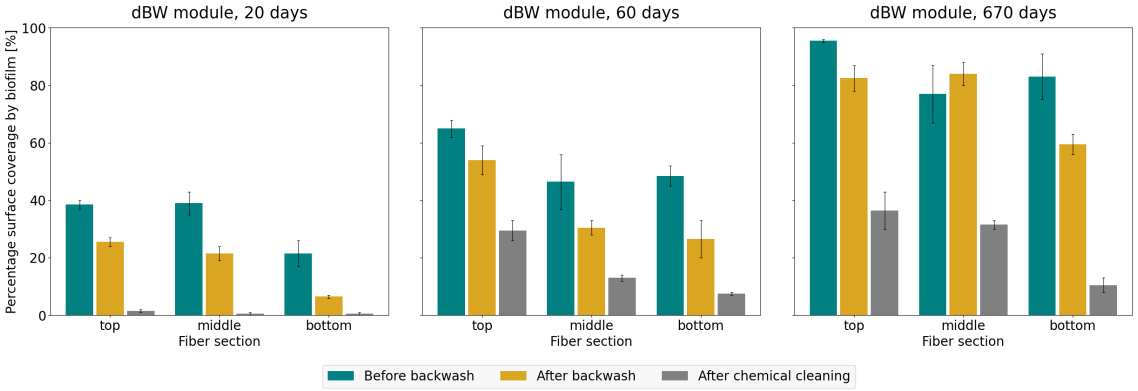

Figure 3.8: Evolution of coverage ratio of dBW module operated for different times

Fig. 3.8 shows the coverage ratio dBW modules with different operational time. It is clear that the coverage ratio before backwash was increasing with time for all 3 sections of one fiber. Moreover, it is also a trend that the coverage ratio decreased from top to bottom sections, before and after backwash, and after chemical cleaning. This dynamics is associated with the trend observed in Fig. 3.6.

3.1.3 biofilm characterization

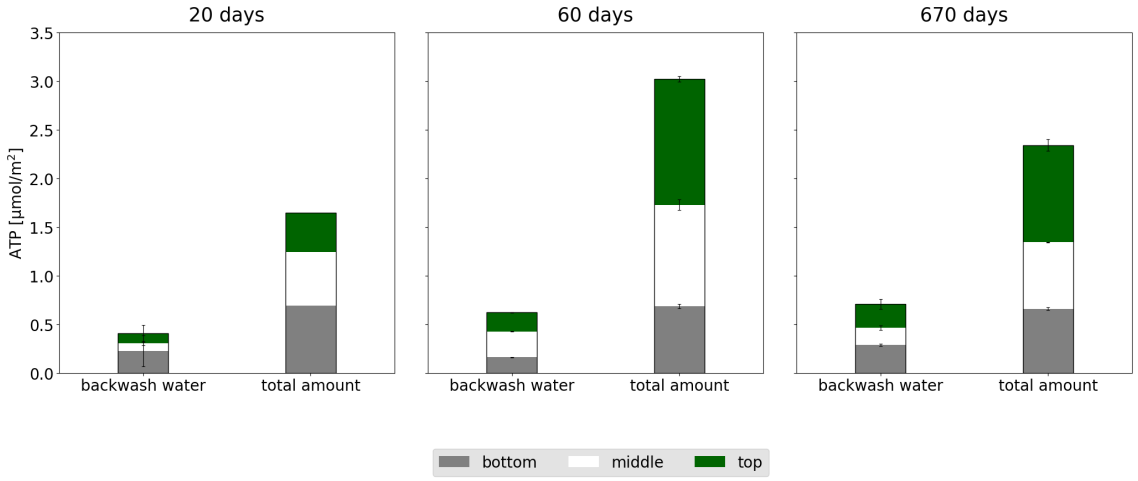

Figure 3.9: ATP of inside biofilm from dBW modules operating for 20, 70 and 670 days. ATP is measured with the method described in subsection 2.6.2

Fig. 3.9 shows the ATP of the backwash water and scratched biofilm (literally all the biofilm) collected from each section of dBW module at 20, 60 and 670 days of the operation. The ATP of each section from one fiber is piled up to represent the ATP of the whole fiber. It can be seen that ATP from backwash water was always less from the scratched biofilm, which means that the backwash was not effective at removing all the biofilm, as it was observed in Fig. 3.6. This is also associated with the coverage ratio. Although it decreased after backwash, it did not decrease to 0. The p-value between coverage ratio and resistance is 0.001506, which means that the evidence against the null hypothesis is strong, thus one hypothesis is that the coverage ratio is the cause of high resistance, since the more biofilm was observed, the high resistance could be expected.

To be noticed that, according to the result of multicorrelation shown in Fig. 3.7, ATP_BW and ATP/TOC_total have a negative correlation. This could be explained that backwash removed a large portion of live cells, but the dead cells were still in the fibers, thus when ATP_BW was high, ATP/TOC_total was low.

But as shown in Fig. 3.9, the total amount of biofilm scratched from dBW_60 was more than that of dBW_670, which did not correspond to the resistance and flux. This needs to be explained with Fig. 3.10.

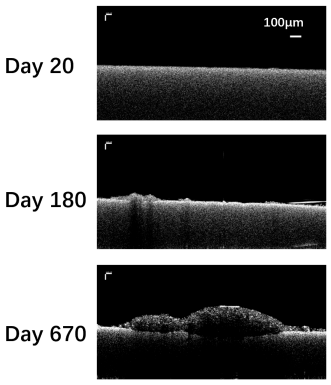

Figure 3.10: Biofilm evolution inside the HF membrane.

Fig.3.10 shows the section view of dBW_20, dBW_60 and dBW_670 modules' inner surface, and provides the relative thickness of each of them. It can be observed that within long time of operation, there were thicker biofilm accumulated on the inner surface and this may be the explanation for the flux drop and resistance increase. Research from Li et al. (20) shows that pure water backwash removes only 33.4% of resistance, while biofouling resistance only accounts 5.3–56.0% of total fouling resistance. This means there is always remaining biofilm and its resistance. Thus the ATP result shown in Fig. 3.9 cannot represent the biofilm resistance as it only shows the amount of live organisms, but fail to consider the total biofilm (live or dead) accumulated inside. To explain the lower ATP of the dBW_670 scratched biofilm, one hypothesis is that there was less live but more dead biofilm accululated, so it had a slightly lower ATP value but a big resistance and low flux. In conclusion, there was a gradient that depends on the backwash frequency and the time; at the top section, there was more biofilm, and with long time accumulation, it was even more. The more biofilm indicated high resistance and lower flux.

3.2 Influence of feed strategies, backwash frequency and high turbidity on flux

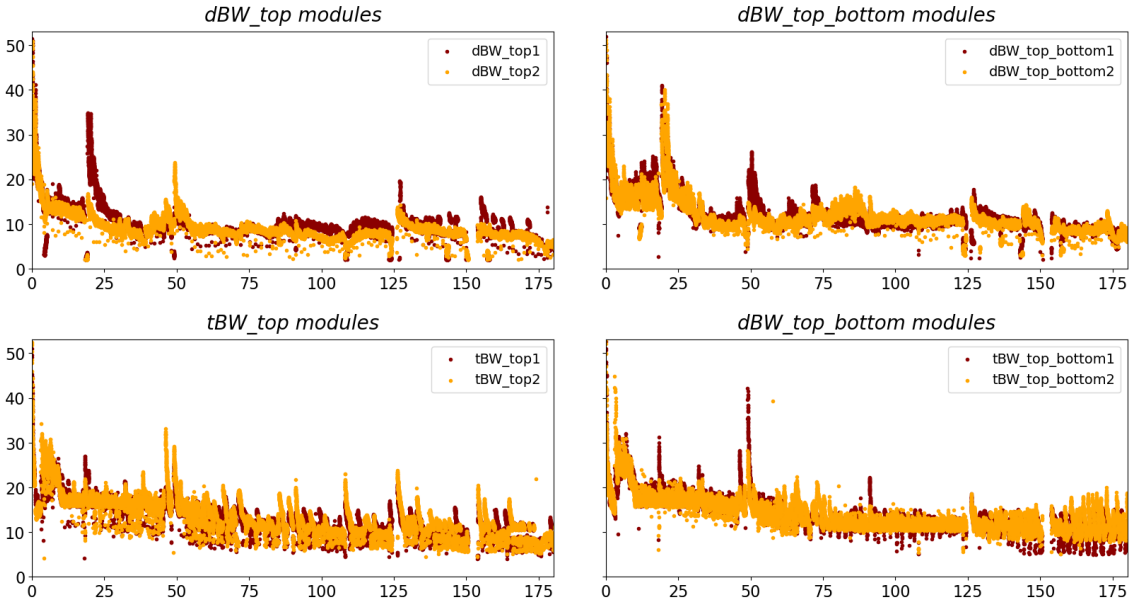

Figure 3.11: Flux of dBW_top, dBW_top_bottom, tBW_top and tBW_top_bottom modules operating for 180 days

Fig. 3.11 shows the modules with different feed strategies (top and top_bottom) and backwash frequency (daily and based on a fixed threshold value). Each feed strategy and backwash frequency

has 2 modules and both of their fluxes are plotted on the same figure. In the last five days of operation (from day 180), the average stable flux of dBW_top, dBW_top_bottom, tBW_top and tBW_top_bottom modules was equal have a flux of 4.5 ± 1.1 L/m^2/h, 7.6 ± 2.5 L/m^2/h, 6.8 ± 4.4 L/m^2/h and 10.2 ± 4.9 L/m^2/h, respectively. Compared to the result from Boller (4) which was measured at day 107, the flux for all 8 modules decreased after another 73 days of operation. In a former study, the stable flux value calculated at day 107 was equal to 8.6 ± 1.4 L/m^2/h, 11.0 ± 2.1 L/m^2/h, 13.6 ± 3.9 L/m^2/h and 13.9 ± 3.4 L/m^2/h, for dBW_top, dBW_top_bottom, tBW_top and tBW_top_bottom, respectively. It can be seen from Fig. 3.11 that there were incidents at day 125 and 152, both of which may lead to the flux drop in long term operation. In fact, at day 151, the canal was dry. There was a heavy rain and the coarse filter was blocked by the particles brought in by the high turbidity water, and there was no water fed to the feed tank until the end of day 152, when the filter was manually cleaned.

Similar conclusion as Boller (4) had that top_bottom feed strategy helped the flux to maintain at a high level, which was 28.2% higher than the top feed in her cases, but 83.4% higher in this research. This value is higher than the one from Boller, this can be explained that long time operation magnify the difference. As to threshold backwash modules however, it was observed that tBW_top module couldn't maintain its flux at the threshold even after the backwash. It also confirms that top_bottom feed is interesting to maintain high flux values. This is also predictable according to the research from Boller (4) that the flux of threshold module decreased gradually from 15 to 10 L/m^2/h and expect the flux could be maintained at a certain level but failed. Even though threshold backwash is not the optimized maintenance, it is still interesting to see its inside biofilm development as well as its resistance, since these may be the reason for its failure.

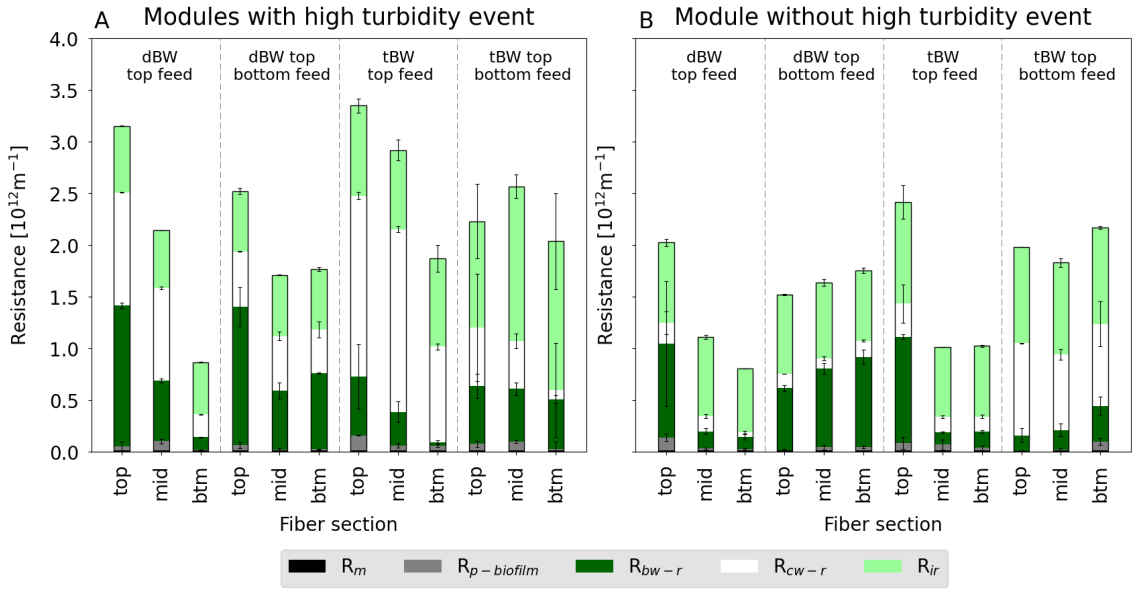

Figure 3.12: Resistance of dBW_top, dBW_top_bottom, tBW_top and tBW_top_bottom modules operating for 180 days. Resistance is measured with the method described in section 2.3

Comparing to dBW_ top and tBW_top modules, dBW_top_botom and tBW_top_bottom modules had a relative homogeneous resistance along the fiber as shown in Fig. 3.12. This trend is in line with the resistance of dBW_20, dBW_60 and dBW_680 modules shown in Fig. 3.6, that the permeate inlet end accumulated more particles than the other end which led to the high resistance

at the inlet and low resistance at the other end. Top bottom feed modules were fed from both ends thus both ends accumulated particles and had similar resistances. As to the dBW_top_bottom adn tBW_top_bottom modules without high turbidity (high turbidity will be explained later in section. 3.2.1), the resistance of both ends seamed similar to their middle section, this may indicate that the biofilm was equally distributed along the fiber, but this will be further discussed in Fig. 3.14. It is expected that if the fiber is longer, the resistance of the middle section will be much smaller than top and bottom sections, but according to the result in Fig. 3.12, it is hard to say if there is a similar gradient for all 4 top_bottom feed modules as they had different trend.

As to their flux value, one could find out the the flux value is not associated with the resistance. For instance, the flux of tBW_top module was 6.8 ± 4.4 L/m^2/h and dBW_top was 4.5 ± 1.1 L/m^2/h, while the resistance of both were similar. One could argue that the standard deviation of the tBW_top module flux is too big, but another explanation is that tBW_top module was backwashed too often, the time it was sacrificed was not long after the previous backwash, which helped the module to recover the flux, and the resistance results in Fig. 3.12 only represent the instant resistance when the fiber is sacrificed.

Fig. 3.13 shows the multicorrelation between all the data included in section. 3.2. Similar to the multicorrelation in section. 3.1.2, the coverage ratio and ATP_total has relative higher correlation with resistance. The p-value between resistance and coverage ratio is as low as 1.75×10^{-7}. Thus both of the data will be discussed. To be noticed that, not like the results shown in Fig. 3.7 in section. 3.1.2, in which the particle size only has slightly negative correlation with resistance, the particle size in Fig. 3.13 has stronger negative correlation with resistance and coverage ratio. This can be explained that large particles formulate the basis of biofilm, with which small particles and cells can then attach to the existed biofilm. Therefore, when the coverage ratio is low, there was not too much biofilm on the fiber, and the existed bilfilm attached to each other to form a large particle. With long time of operation, more small particles and cells came and attached to the previous large biofilm, and the average size of the biofilm was decreased.

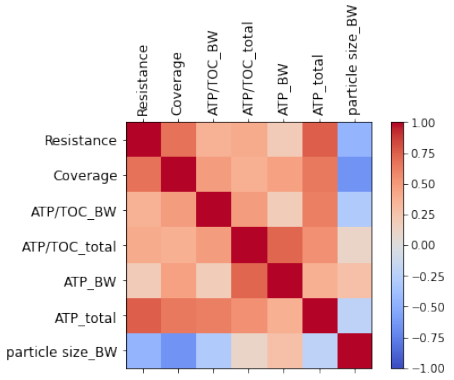

Figure 3.13: Multicorrelation of different data

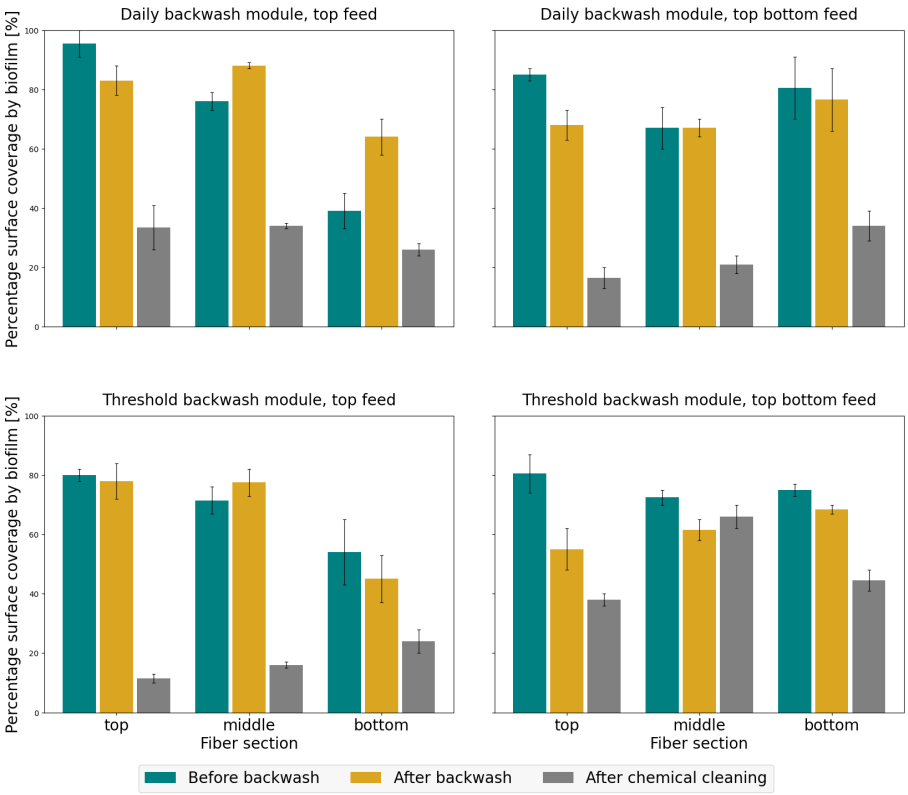

Figure 3.14: Coverage ratio of inside biofilm of dBW_top, dBW_top_bottom, tBW_top and tBW_top_bottom modules operating for 180 days. Coverage ratio is measured with the method described in subsection 2.5

Similar to resistance shown in Fig. 3.12, the coverage ratio also shows that top_bottom feed modules had quite homogeneous coverage ratios along the fiber while the top feed modules had high coverage ratio at the feeding end but low at the other end, and this trend works both on dBW and tBW modules. According to the results from section. 3.1, a similar trend is found on the modules fed from one end. This confirms that the closer the distance to the feeding end is, the higher the coverage ratio would be, because the feeding end had more food which thrived the biofilm.

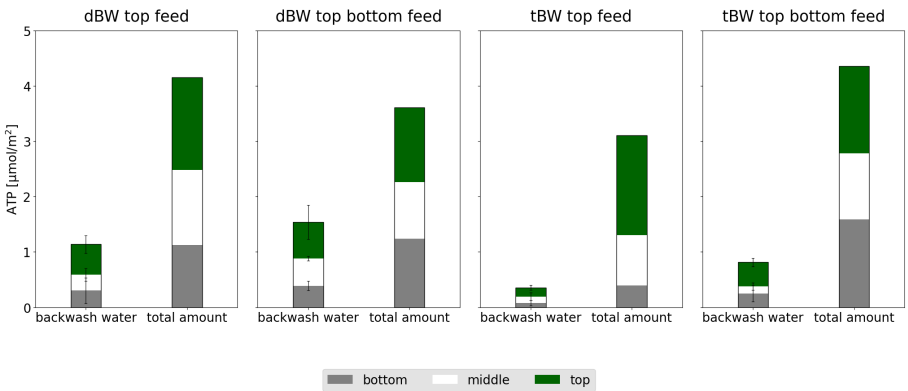

Figure 3.15: ATP of inside biofilm from dBW_top, dBW_top_bottom, tBW_top and tBW_top_bottom modules operating for 180 days. ATP is measured with the method described in section 2.6.2

Fig. 3.15 shows the ATP of the backwash water and scratched biofilm collected from each section of dBW_top, dBW_top_bottom, tBW_top and tBW_top_bottom modules operating for 180 days, with the method mentioned in section. 2.6.2. ATP of each section from one fiber is stacked to represent the ATP of the whole fiber. Similar to the results from Fig. 3.9, ATP from backwash water was always less from the scratched biofilm, and this become more apparent to tBW_top and tBW_top_bottom modules. Research from Dai et al. and Desmond et al. (22; 9) show that the more backwash is applied the more EPS is preserved in the biofilm, which then leads to a lower backwash efficiency.

3.2.1 High turbidity event

High turbidity events were simulated to test the resilience of the modules with different feed strategies and backwash frequencies. The turbidity during the events are shown on Fig. C.1 and Fig. C.2 in the Appendix. C. The experiment was carried out during 3 weeks before sacrificing the module at around day 210, so that the flux of each module from day 0 to day 180 was not disturbed by the high turbidity. However, Boller carried out high turbidity event around day 60 to 70, but her result showed that after rapid backwash, the flux of all modules were recovered, so the influence can be ignored.

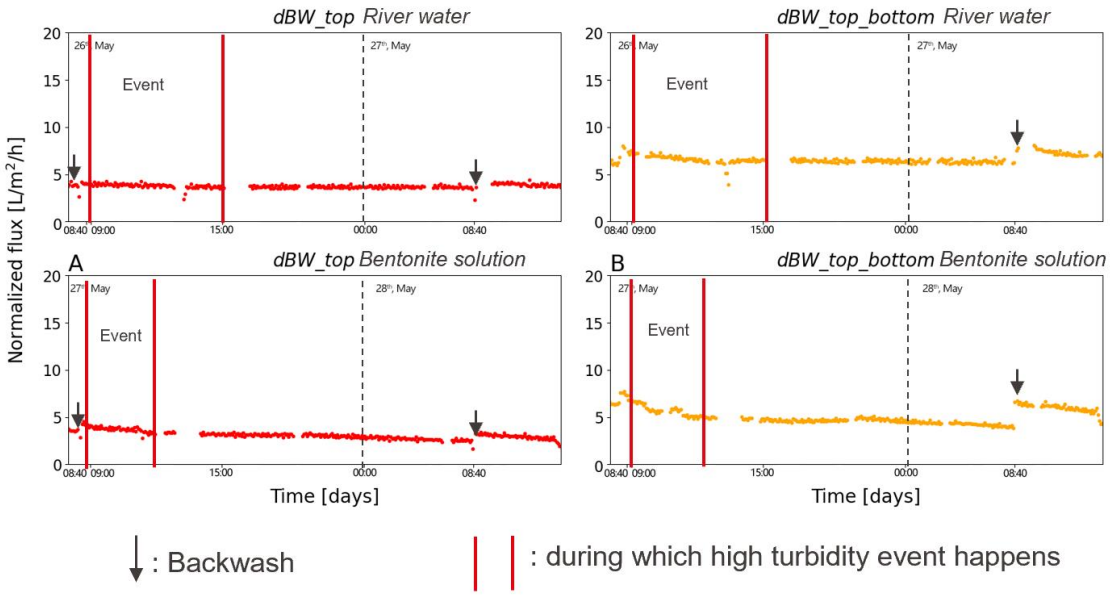

Figure 3.16: Flux of dBW_top and dBW_top_bottom modules before, during and after the high turbidity event

Fig. 3.16 gives the flux of dBW_top and dBW_top_bottom modules before, during and after the high turbidity event. The black arrows point the time when backwash occurred. Flux drop of 0.0217 $L/m^2/h$ and 0.104 $L/m^2/h$ in 6 hours was observed for dBW_top and dBW_top_bottom modules during the river water high turbidity event; flux drop of 0.0433 $L/m^2/h$ and 0.412 $L/m^2/h$ in 3 hours was observed for dBW_top and dBW_top_bottom modules during the bentonite solution high turbidity event (the values were calculated with the flux value in 5 minutes before and after backwash). The flux drop of all modules were not significant during both river water and bentonite simulation high turbidity events, as each module had a normal flux around 5 $L/m^2/h$. After the

next day's backwash, all modules had a flux recovery more than 95%, except for dBW_top_bottom module, for which the flux recovery was 87.1%. This result is quite surprising because according to previous results, top_bottom feed is always the better feed strategy as it had high flux, but after going through the high turbidity event, it was not recovering well by the first backwash. One explanation could be that since top_bottome feed modules had two inlets, there are more particles going into the module and hindering the filtration, which led to a larger flux drop; Since the backwash had the same duration for every module, it is likely that the modules with more particles were less thoroughly cleaned during a certain backwash, and this led to a lower flux recovery.

Moreover, bentonite high turbidity simulation provided a larger flux drop and lower flux recovery to modules irrespective of the feed strategies. This could be explained with the particle size of the used materials. The river water had an average particle size of 69.3 μm while bentonite was 4.5 μm. The research of Koyuncu et al. says that larger particles are difficult to get inside of the module and easy to be cleaned by backwash, while the small ones are not (13). So, this provides an explanation to the different flux drop and flux recovery.

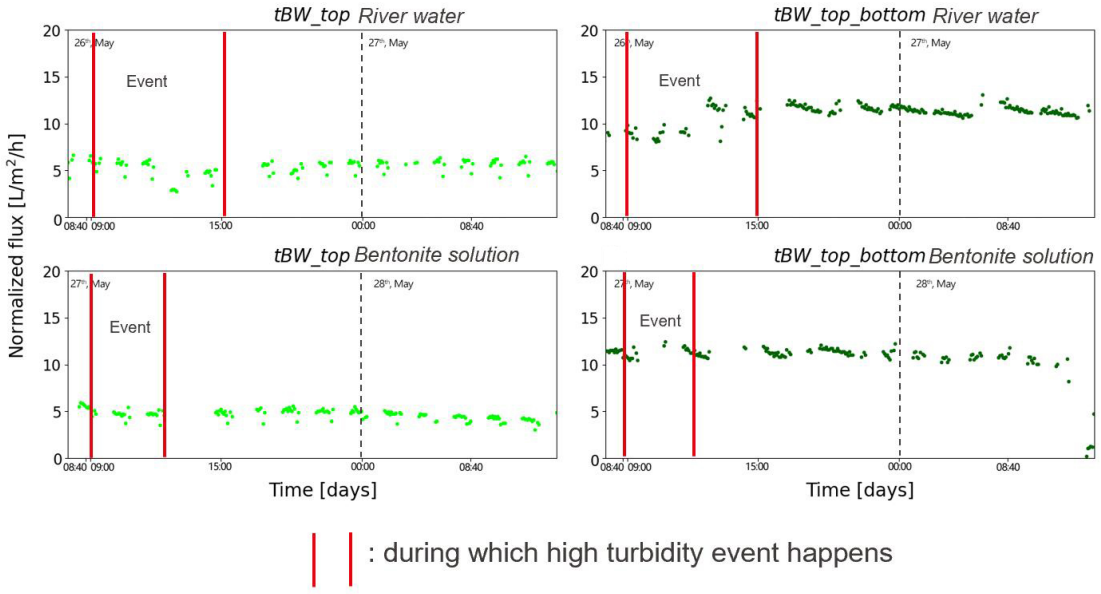

Figure 3.17: Flux of tBW_top and tBW_top_bottom modules before, during and after the high turbidity event

Fig. 3.17 provides the flux of tBW_top and tBW_top_bottom modules before, during and after the high turbidity event. Since several backwashes occurred during and after the high turbidity events, the times of backwashes were not indicated on the figure. Flux drop of 0.0677 L/m^2/h in 6 hours was observed for tBW_top module during the river water high turbidity event; flux drop of 0.022 L/m^2/h in 3 hours was observed for dBW_top module during the bentonite solution high turbidity event. As to the tBW_top_bottom modules, its flux even increase during the event since there was backwash happening simultaneously. The flux drop is not relevant since they were too small. As to the flux recovery, since a lot of backwash happened, the flux after the first backwash after the high turbidity event was equal or even higher than the one before the event, so all 4 modules had a recovery of 100%. This result is much more comparable to the previous flux and

resistance results of the associated modules. Under the same backwash threshold (10 L/m^2/h), modules fed from top and bottom had high flux, as well as resilience during the extreme event.

Comparing the dBW_top and tBW_top module, it can be concluded that tBW_top had a higher flux recovery. This can be interpreted with the number of backwash cycles that happened during the event. Fig. 3.18 shows that 3 backwashes happened during the event. Apparently, threshold backwash is the better way to ease the flux drop during high turbidity events since it is backwashed when the flux is low (when the module is clogged enough).

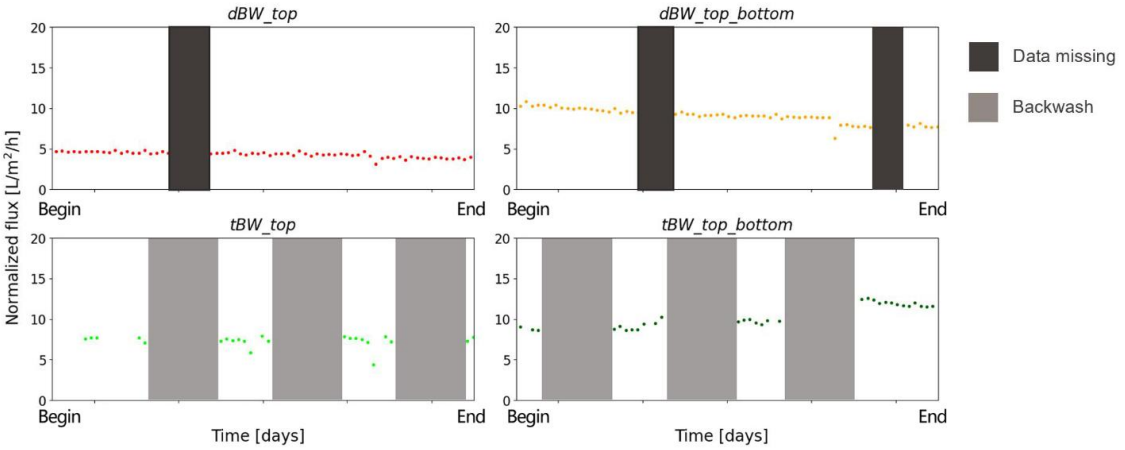

Figure 3.18: Flux of tBW_top and tBW_top_bottom modules during the high turbidity event

As a conclusion, particles with size from 4.5 to 69.3 μm cannot provide a significant flux drop to modules with different maintenance (daily backwash and threshold backwash) and feed strategies (top and top_bottom feed). tBW module is more resilience during high turbidity event comparing to dBW module, but there will be less difference between their flux after the first backwash of dBw module after the high turbidity event.

3.3 Link between backwash water quality and permeate quality

When observing the permeate side of the membrane with LM, it was visible that a biofilm grew; the higher the operation time, the more the biofilm (Fig. 3.19), while there was almost no bioflim on the nBW module. Contrary to the inside biofilm that showed a gradient along the fiber, the outside biofilm seemed to be homogeneously distributed along the fiber. This phenomenon indicates that the outside biofilm may not be largely impacted by the feed water but the quality of water used for backwash since permeate was used for bachwash after it was stored in the backwash tank, and the backwash tank was not disinfected. Boller also showed that there were cells in the water for backwash (4).

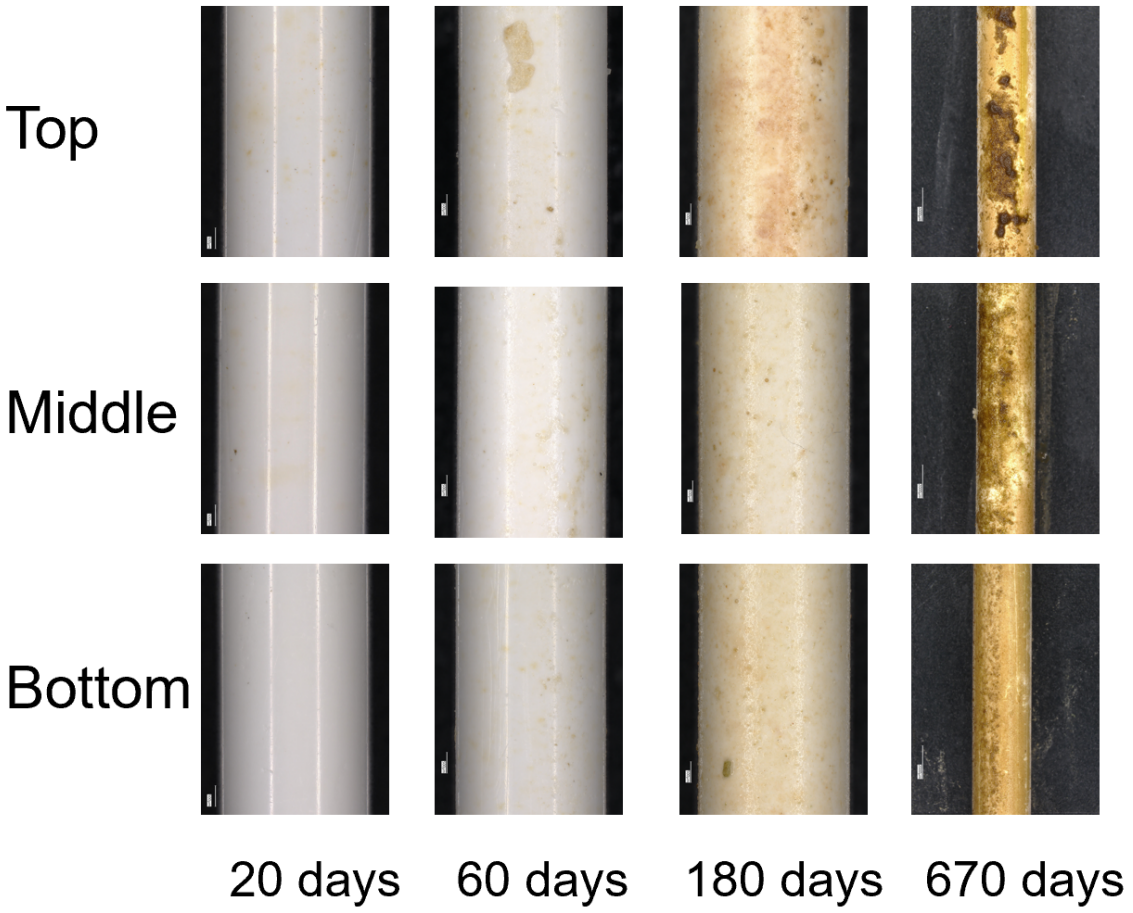

Figure 3.19: LM pictures of the outside surface of dBW_20, dBW_60, dBW_180 and dBW_670 modules at 20, 60, 180 and 670 days of operation

During the backwash, the permeate brought the cells inside the module and the backwash flux pressed the cells against the permeate side of HF membrane, after that, some cells attached to the outside of HF membrane permanently and slowly constituted a biolfilm with the continuously supplied AOC in the permeate (25). As described in section. 3.1.1 and section. 3.1.2, the outside biofilm contributed little (mostly less than 10%) to the total resistance of membrane, but it may be a problem to the permeate quality. According to the results from Boller (4), their was a leap of TCC soon after backwash, and this indicate the backwash is connected to the permeate quality soon afterwards. To better understand the relationship between backwash, outside biofilm and the permeate quality, 4 modules with different water for backwash were operated for 21 days, as descibed in section. 2.6.4.

Fig. 3.20 shows the quality of the solutions used for daily backwash right after preparation and the quality of the permeate collected for the backwash. Manually prepared solutions showed low levels of cells concentration (all less than 1000 cells per mL), which means that water for backwash was sterile, and was expected to have a negligible impact on the inoculation of cell in the permeate side of the membrane. When the backwash water was permeate, the TCC concentration continuously increased during the 21 days that the experiment lasted. This increase could be explained by the fact that the backwash tank that contained the permeate was disinfected with NaOCl at 200 mg/L before the experiment (no residual chlorine remained). Despite disinfecting and covering the backwash tank, regrowth occurred until reaching 3.49 ± 0.11 $\times 10^4$ cells/mL at day 21. The reason for its increase will be discussed later with Fig. 3.24.

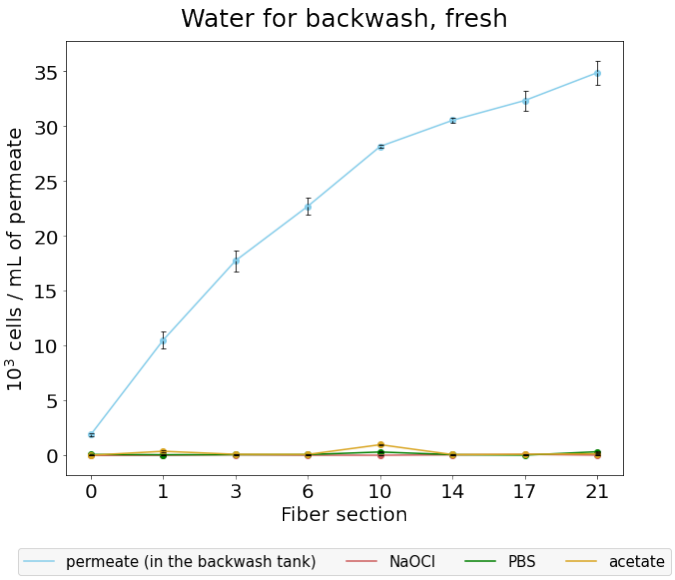

Figure 3.20: TCC of water for backwash soon after its prepared.

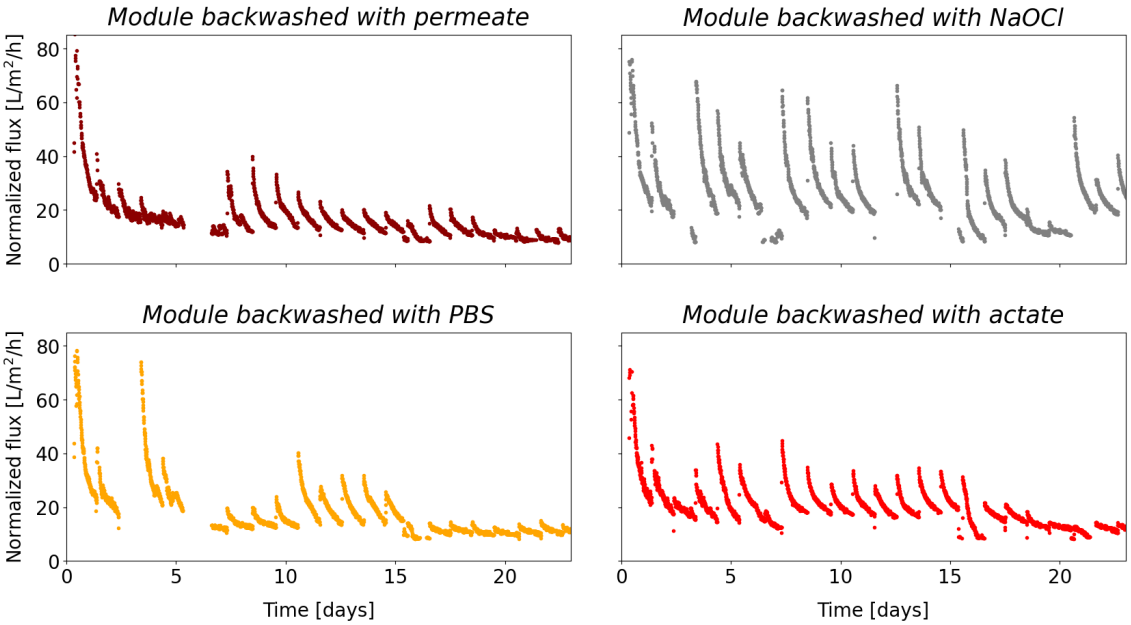

Figure 3.21: Flux of 4 modules backwashed with water of different quality.

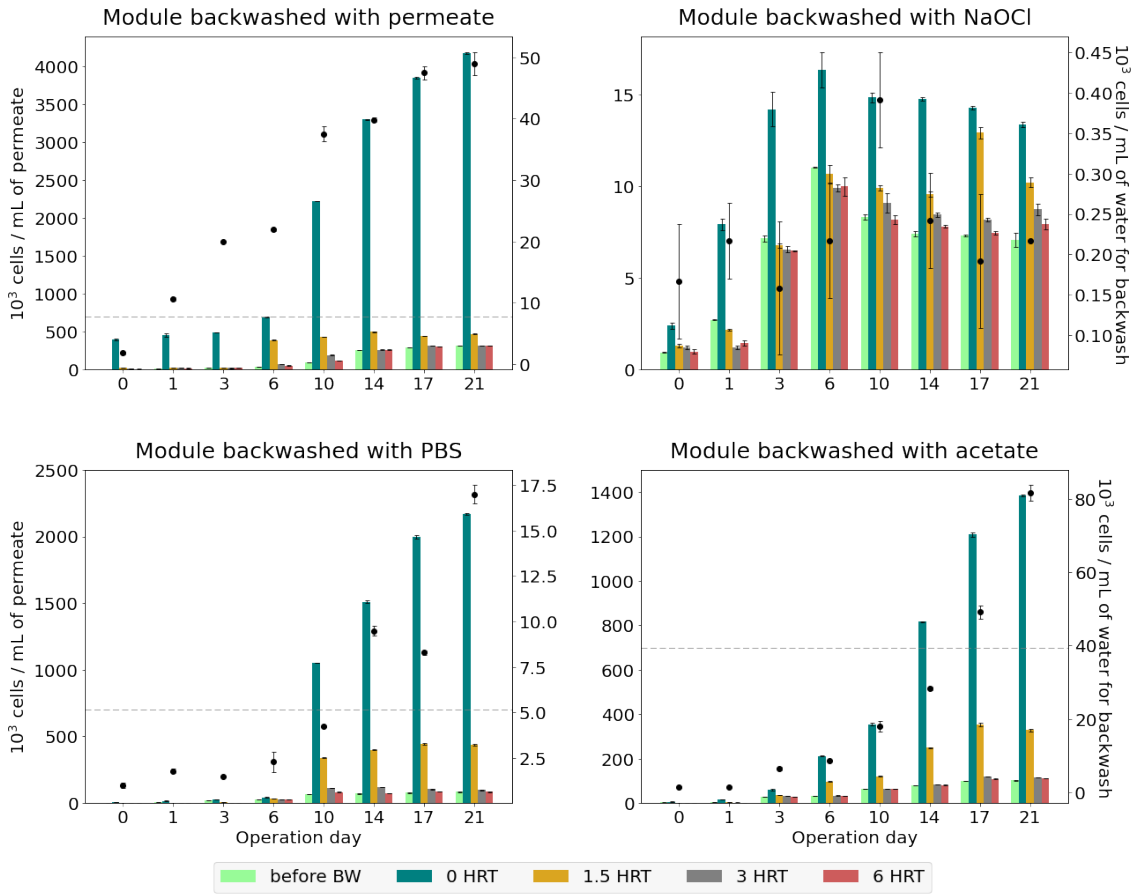

Figure 3.22: TCC of permeate and water for backwash after going through the tubes and valves, before entering the module. Each dot indicates the change of TCC of water for backwash. The sample was taken from the tube connecting module and backwash tank, this means that the water for backwash had gone through the tubes and valves, which may be contaminated

Fig. 3.22 shows the quality of permeate (represented by the bars), and water for backwash after going though all the pipes and valves and before entering the modules (represented by the scatters). The dash grey line represents the influent TCC at 7×10^5 cells/mL (this is the same for all modules). As to the water for backwash, at day 0, the backwash tanks and valves have been disinfected with 200 mg/L NaOCl (immersed in NaOCl solution for 24 hours) and all the pipes were sterilized, and this was why the TCC of water for backwash after going though valves and tubes was at a low level at day 0. After the start up of operation, the concentration in cells of the manually prepared PBS and acetate solutions increased considerably when going through the system and before entering the module, in comparison to the concentration measured after preparation (Fig. 3.20). This means that bacteria present in the pipes and valves contaminated the manually prepared solutions. For both PBS and acetate solutions, the concentration increased with time, showing that there is also regrowth in the pipes. This is striking for the acetate solution, where the TCC exponentially increased by a factor of 1000 in 21 days. This exponential increase could be explained by acetate as substrate for regrowth. Actually, the regrowth in the pipe has already been observed by Hammes et al. (14), that regrowth even occurs to the stagnated drinking water in household taps overnight. NaOCl solution did not have the same trend, while its TCC remained at a relatively low lever (around 250 cells/mL of solution) for the whole time. This can be explained by disinfection of the

chlorine. As to the TCC in the permeate, at 0 HRT it was increasing as a function of time for the module backwashed with PBS, acetate and permeate. Even though the TCC levels of permeate was much high than that of water for backwash, the dynamic can still be seen that the permeate quality at 0 HRT was changing with the quality of water for backwash. As to the permeate of module backwashed with NaOCl, its TCC increased at the first 3 days but then remained at the level around 1.4×10^4 cells/mL for the rest of the time, and this trend is also similar to its water quality of backwash. To be noticed that apart from the TCC at 0 HRT, no permeate at other HRTs had higher TCC than the influent (indicated by the dash grey line), which means that the biofilm at the permeate side was not really a problem.

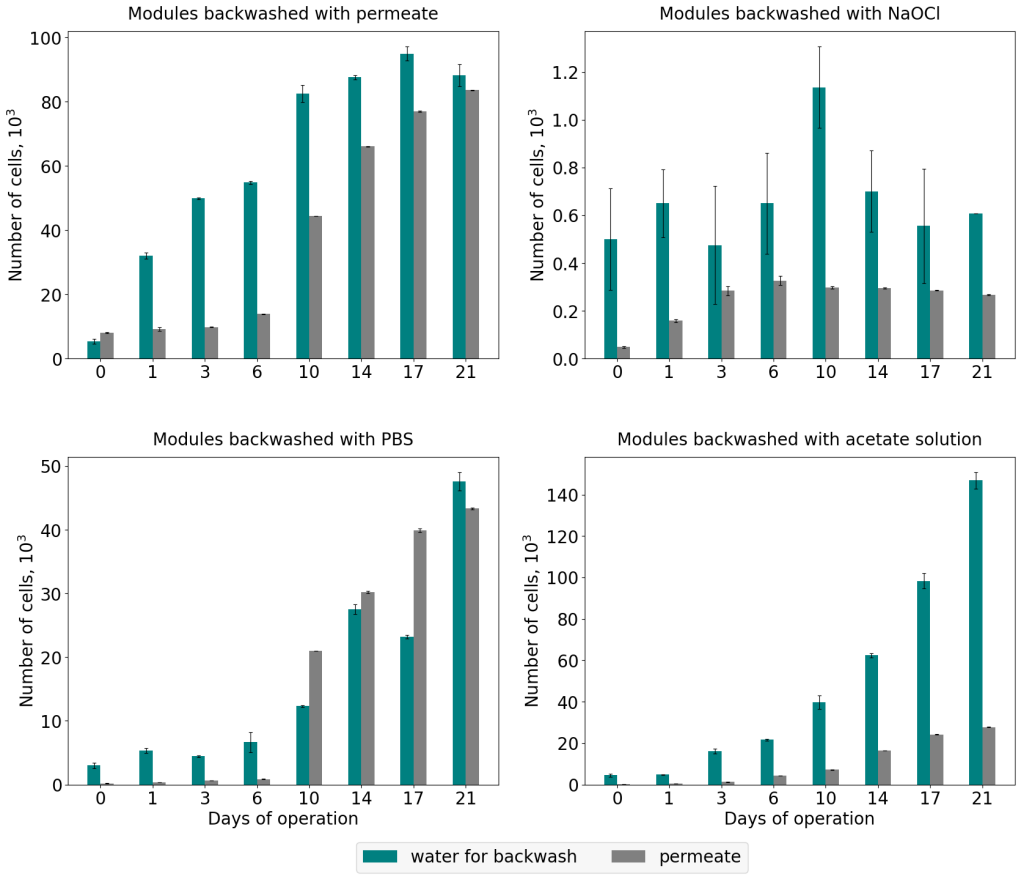

Figure 3.23: Accumulation TCC into the module during the backwash and the flush out of cells during filtration.

As described in previous paragraph that the TCC of permeate at 0 HRT was increasing with the TCC of water for backwash, although they are at different magnitude, one could come up with the hypothesis that the value of each are correlated. Fig. 3.23 shows the TCC (the total amount of cell, not concentration) of water for backwash and its corresponding permeate quality. The total number of cells in the permeate is calculated with the concentration of the permeate and its volume, which is 20 mL for each samples (20 mL is the size of one kind of glass bottle); the total number of cells in the water for backwash is calculated with its concentration and volume, and the volume is estimated with other dBW modules (this calculation wasn't planed, so there was no data for the amount of backwash water modules need, but there are data from other dBW modules, whose backwash water was collected and weighted). A dBW module needs approximately 3 L of water

for backwash at the beginning of the operation, and the amount drops to around 2 L after 3 weeks (these data is from the daily measurement of backwash water volume of dBW_20 and dBW_60 modules). It can be seen that for all 4 modules the TCC of water backwash was much higher than that of permeate, but this gap narrowed at about 10 days of operation for module backwashed with permeate and PBS, while the gap still exists for module backwash with acetate and NaOCl solution. This may indicate that for the first 10 days, there was a biofilm development on the outside of the HF membrane, thus a lot of cells went inside the modules with backwash but less went out. After 10 days, the biofilm for module backwashed with PBS and permeate became stable. The research from Peter-Varbanets et al. (17) shows that the biofilm remained homogeneous from the 7^{th} day, which is similar to what presented by the TCC result. The module backwash with NaOCl always had residual chlorine in the water for backwash, thus the cell number kept on decreasing during backwash and the filtration afterwards, thus the TCC of permeate was always lower than that of water for backwash. The module backwashed with acetate had continuously food supply for the outside biofilm, so up until day 21, the biofilm was still developing, and this led to the gap between TCC value of water for backwash and permeate.

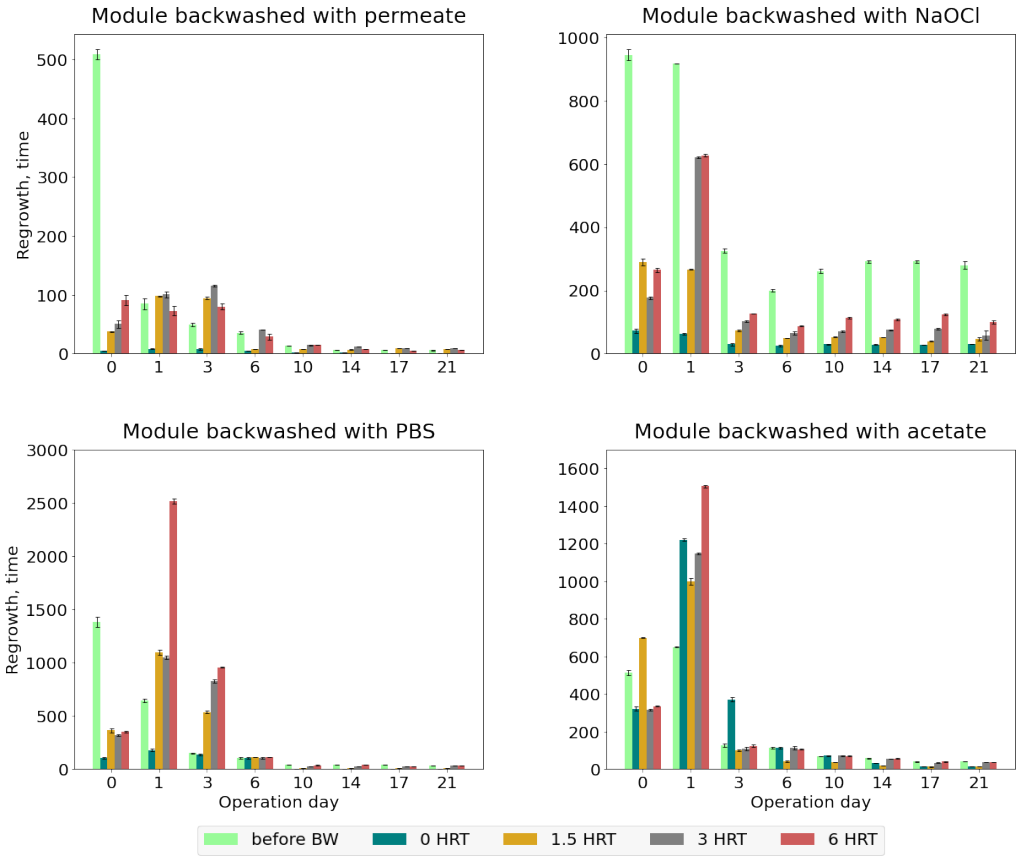

Figure 3.24: egrowth of cells in permeate for different HRT.

Fig. 3.24 shows the regrowth potential of each sample described in Fig. 3.22. For all the modules, in the first days of filtration, the regrowth was important before backwash. There was nutrient available (7) but almost no cell provided on the ouside of HF membrane, so a large amount of nutrient plus a few cells means huge regrowth at the beginning . After longer operation time, the regrowth before backwash was lower, while the TCC was higher. It is expect more AOC to be removed by the inside biofilm so less AOC was provided to outside biofilm. As a consequence, the

regrowth decreased. Generally, in contrary to TCC, the regrowth was high when the TCC was low. This trend is suitable for modules backwashed with PBS, acetate and permeate. The module backwash with NaOCl, its regrowth of permeate at 0 HRT decreased and became stable after 3 days operation, which is the same time that the corresponding TCC reached its plateau shown in Fig. 3.22.

As a conclusion, there is always cells and regrowth in the permeate, no matter the quality of the water for backwash, but continuous chemical cleaning can stabilize the regrowth. Moreover, high initial TCC value refers to low regrowth and vice versa. This may suggest that users of GMD must toleratea certain level of cells in the permeate if they did not expect a high regrowth. Chemical disinfection works, but only at the moment it is implemented. Continuous chemical disinfection is needed if one expected low cell concentration in the permeate as well as low regrowth.

Chapter 4

Conclusion

The present study aims at investigating the inside biofilm distribution development of inside-out operation HF membrane in GMD mode. Moreover, modules with different feed strategies and maintenances are investigated find the one with highest permeability. Modules with different feed strategies and maintenances are also studied to see their resilience to high turbidity event in terms of flux and flux recovery. Finally, the influence of water for backwash on the permeate quality is studied. The following 6 points are the conclusions of the finding in this study:

1.A more pronounced gradient of biofilm distribution on the inside (influent side) of the membrane was found within the decreasing backwash frequency (daily backwash, weekly backwash and no backwash) in 3 weeks of operation;

2.Resistance distribution study showed that there is a biofilm gradient on the inside (influent side) of the membrane, and it develops with time;

3.Changing the feed from top to top-bottom allows to redistribute biofilm along the fiber and use more membrane surface. This increases the overall flux and productivity. However, the threshold is redistributing, but with much higher resistance due to too frequent backwash. Plus its productivity is low. This is not a good approach. To increase the flux, top-bottom is an interesting approach;

4. Threshold backwash is a better approach to maintain the flux during the high turbidity event compared to daily backwash. Threshold backwash modules are backwashed on needs and tolerate no flux lower than the predetermined level;

5.There is a TCC peak soon after backwash. It is due to the residual bacteria in the valves and tubes. During the backwash, the water for backwash brings these cells into the module, and these cells are flushed out with permeate after backwash. It is difficult to keep the permeate free from cells;

6.High regrowth achieved by low TCC, but low regrowth is achieved by high TCC in the permeate. When there is a disinfection in the backwash, the regrowth remains high. This means that letting bacteria inside the permeate is increasing the biological stability and the outside biofilm is useful to stablize the permeate quality.

However, there are a few areas that can be improved with further study:

1. High turbidity simulation did not have a homogeneous influent turbidity. The so called high turbidity may only lated for 1 hour out of the 6 or 3 hours of experiment. On explanation would be that the particles settled too quickly despite that there was continuous manual stirring;

2. The study on the influence of quality of water for backwash on permeate quality could be

continued. It can be seen in Fig. 3.22 that the TCC was still increasing within 21 days, but it is expected to reach and stable at a certain level.

Inside-out HF membrane is a good system with limited biofilm growth and promising permeability within short term operation, it would be interesting to carry out more research on it, as I am still surprised by what was observed within half year of study. It is its own configuration that largely limits people's observation on it, as its filtration, as well as its filtration is happening inside of the lumen, which cannot be directly observed by eyes. However, with the study of its permeate quality, and sacrifice some of them to picture their inside biofilm helped to understand its basic mechanism and compare to other membrane, it is promising that one day, people will find a better way interpret its behavior and use it in a proper way.

Appendix A

Details of flux

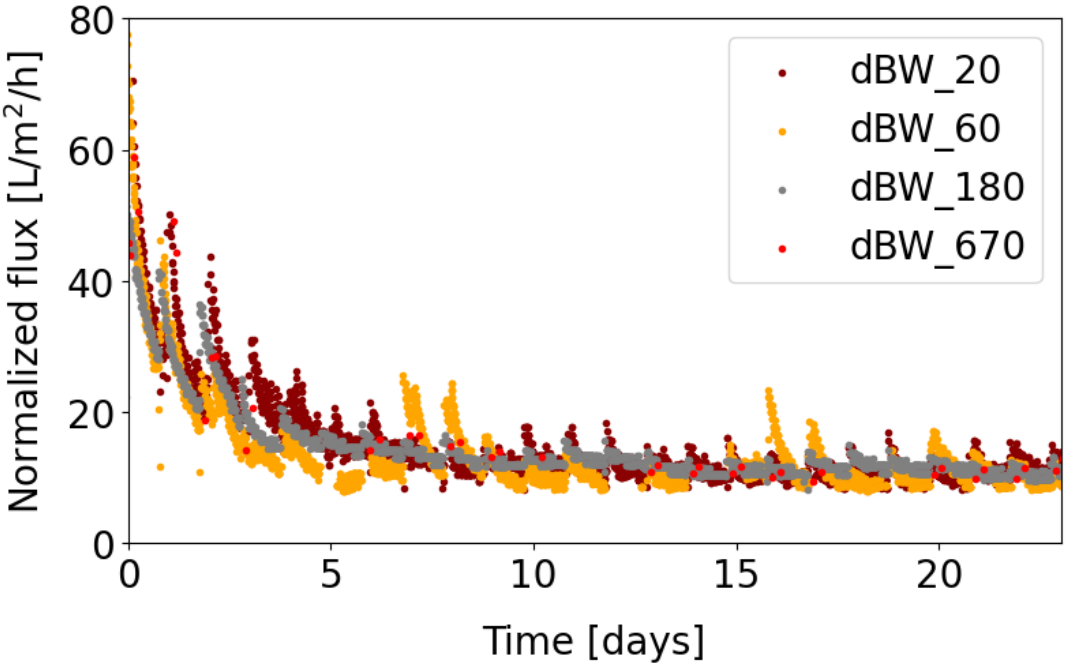

Figure A.1: Evolution of the flux of 4 dBW modules for the first 20 days of operation

Fig. A.1 shows the flux of dBW_20, dBW_60, dBW_180, dBW_670. All of the fluxes are similar within 20 days of operation, which indicates that it is reproducible for dBW maintenance, and each module could be representative for each time stage of one single module.

Appendix B

Permeate quality during the module operation

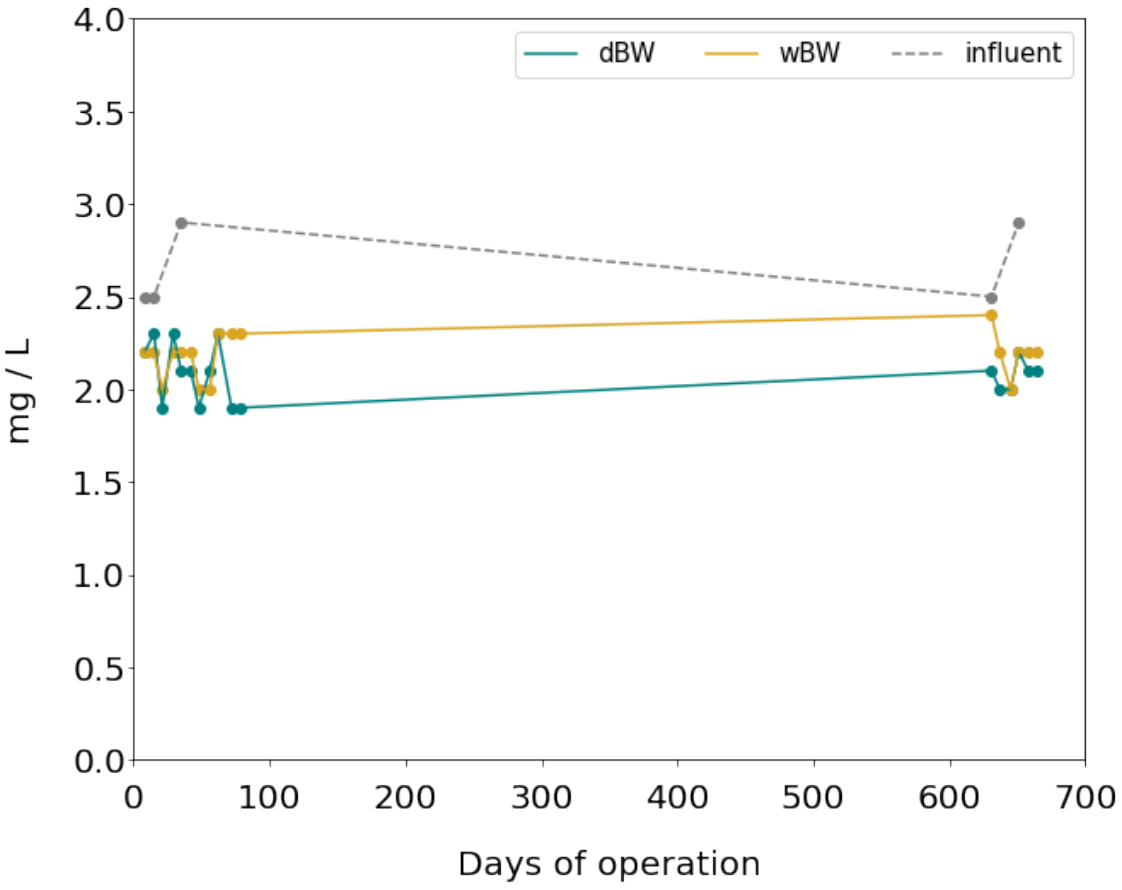

Figure B.1: TOC in permeate of dBW and wBW module during 670 days of operation

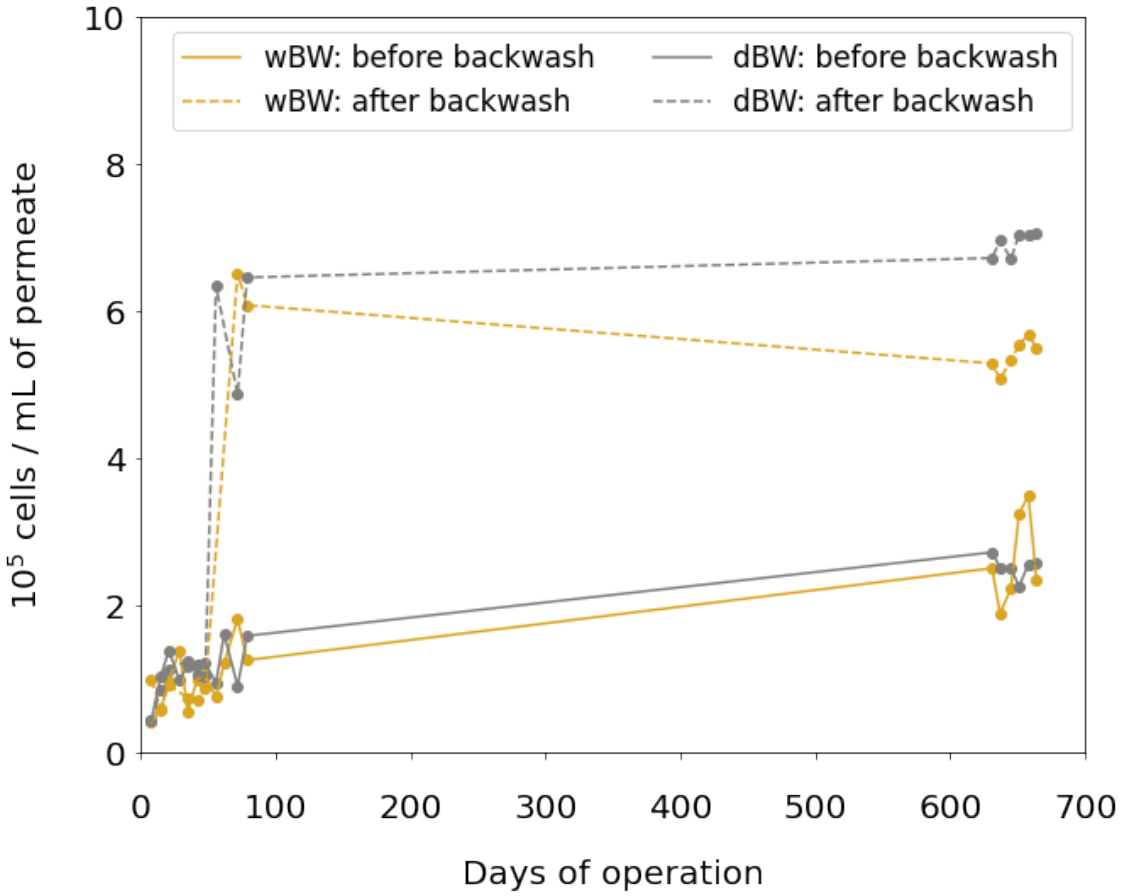

Figure B.2: TCC in permeate of dBW and wBW module before and after bachwash in 670 days of operation

Appendix C

Feed water turbidity during high turbidity event

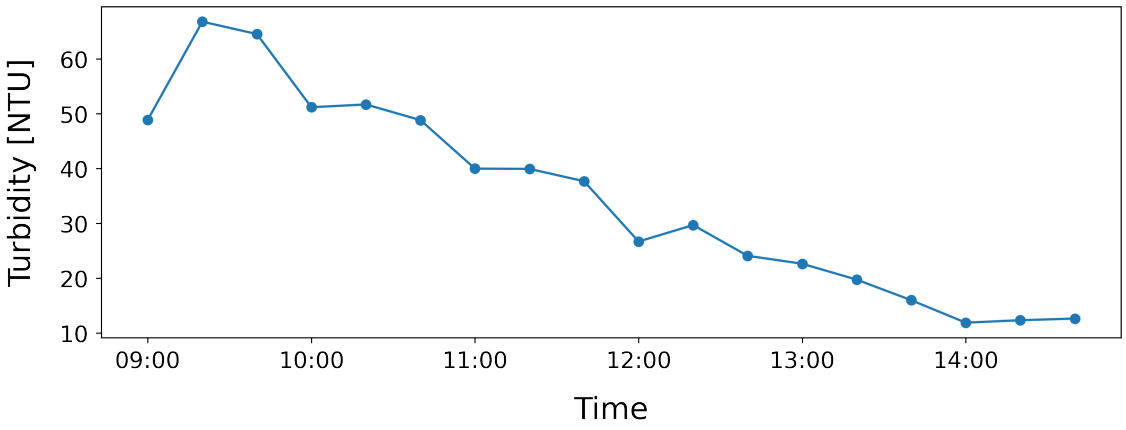

Figure C.1: Turbidity (NTU) of feed water tank during the event (river water 2)

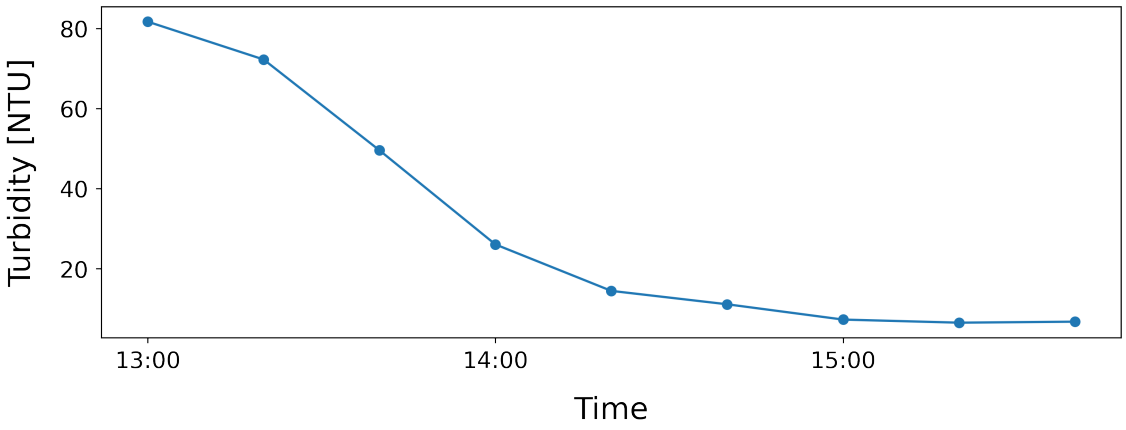

Figure C.2: Turbidity (NTU) of feed water tank during the event (bentonite solution 2)

Bibliography

[ben] Bentonite product. *https://www.sigmaaldrich.com/CH/de/product/sigald/285234*. Accessed: 2022-05-17.

[2] Atkinson, S. (2021). Energy-saving ultrafiltration membrane removes viruses. *Membrane Technology*, 2021(10):7.

[3] Barambu, N. U., Marbelia, L., Bilad, M. R., and Arahman, N. (2021). 9 - gravity-driven membrane filtration for decentralized water and wastewater treatment. In Samui, P., Bonakdari, H., and Deo, R., editors, *Water Engineering Modeling and Mathematic Tools*, pages 177–185. Elsevier.

[4] Boller, M. (2022). Effect of biofilm distribution and influent particles on the performance of gravity-driven hollow fiber membranes operated in inside-out mode.

[5] Derlon, N., Desmond, P., Rühs, P. A., and Morgenroth, E. (2022). Cross flow frequency determines the physical structure and cohesion of membrane biofilms developed during gravity-driven membrane ultrafiltration of river water: Implication for hydraulic resistance. *Journal of Membrane Science*, 643:120079.

[6] Derlon, N., Koch, N., Eugster, B., Posch, T., Pernthaler, J., Pronk, W., and Morgenroth, E. (2013). Activity of metazoa governs biofilm structure formation and enhances permeate flux during Gravity-Driven Membrane (GDM) filtration. *Water Research*, 47(6):2085–2095.

[7] Derlon, N., Mimoso, J., Klein, T., Koetzsch, S., and Morgenroth, E. (2014). Presence of biofilms on ultrafiltration membrane surfaces increases the quality of permeate produced during ultra-low pressure gravity-driven membrane filtration. *Water Research*, 60.

[8] Desmond, P., Böni, L., Fischer, P., Morgenroth, E., and Derlon, N. (2018). Stratification in the physical structure and cohesion of membrane biofilms — implications for hydraulic resistance. *Journal of Membrane Science*, 564:897–904.

[9] Desmond, P., Huisman, K. T., Sanawar, H., Farhat, N. M., Traber, J., Fridjonsson, E. O., Johns, M. L., Flemming, H.-C., Picioreanu, C., and Vrouwenvelder, J. S. (2022). Controlling the hydraulic resistance of membrane biofilms by engineering biofilm physical structure. *Water Research*, 210:118031.

[10] Ding, A., Liang, H., Li, G., Szivak, I., Traber, J., and Pronk, W. (2017). A low energy gravity-driven membrane bioreactor system for grey water treatment: Permeability and removal performance of organics. *Journal of Membrane Science*, 542:408–417.

[11] Göransson, G., Larson, M., and Bendz, D. (2013). Variation in turbidity with precipitation and flow in a regulated river system – river Göta Älv, SW Sweden. *Hydrology and Earth System Sciences*, 17(7):2529–2542.

[12] inge GmbH (2021). inge Ultrafiltration Modules - Multibore® Membranes. https://www.dupont.com/products/multibore.html (Accessed 2 December 2021).

[13] Kaya, R., Deveci, G., Turken, T., Sengur, R., Guclu, S., Koseoglu-Imer, D. Y., and Koyuncu, I. (2014). Analysis of wall shear stress on the outside-in type hollow fiber membrane modules by cfd simulation. *Desalination*, 351:109–119.

[14] Lautenschlager, K., Boon, N., Wang, Y., Egli, T., and Hammes, F. (2010). Overnight stagnation of drinking water in household taps induces microbial growth and changes in community composition. *Water Research*, 44(17):4868–4877. Microbial ecology of drinking water and waste water treatment processes.

[15] Nakatsuka, S., Nakate, I., and Miyano, T. (1996). Drinking water treatment by using ultrafiltration hollow fiber membranes. *Desalination*, 106(1):55–61.

[16] Peter-Varbanets, M., Dreyer, K., McFadden, N., Ouma, H., Wanyama, K., Etenu, C., and Meierhofer, R. (2017). Evaluating novel gravity-driven membrane (gdm) water kiosks in schools.

[17] Peter-Varbanets, M., Hammes, F., Vital, M., and Pronk, W. (2010). Stabilization of flux during dead-end ultra-low pressure ultrafiltration. *Water Research*, 44(12):3607–3616.

[18] Peter-Varbanets, M., Margot, J., Traber, J., and Pronk, W. (2011). Mechanisms of membrane fouling during ultra-low pressure ultrafiltration. *Journal of Membrane Science*, 377(1):42–53.

[19] Pronk, W., Ding, A., Morgenroth, E., Derlon, N., Desmond, P., Burkhardt, M., Wu, B., and Fane, A. G. (2019). Gravity-driven membrane filtration for water and wastewater treatment: A review. *Water Research*, 149:553–565.

[20] Shao, S., Wang, Y., Shi, D., Zhang, X., Tang, C. Y., Liu, Z., and Li, J. (2018). Biofouling in ultrafiltration process for drinking water treatment and its control by chlorinated-water and pure water backwashing. *Science of The Total Environment*, 644:306–314.

[21] Shi, D., Liu, Y., Fu, W., Li, J., Fang, Z., and Shao, S. (2020). A combination of membrane relaxation and shear stress significantly improve the flux of gravity-driven membrane system. *Water Research*, 175:115694.

[22] Siddiqui, M. A., Dai, J., Luo, Y., and Chen, G. (2020). Investigation of the short-term effects of extracellular polymeric substance accumulation with different backwashing strategies in an anaerobic self-forming dynamic membrane bioreactor. *Water Research*, 185:116283.

[23] Singh, R. and Hankins, N. P. (2016). Chapter 2 - introduction to membrane processes for water treatment. In Hankins, N. P. and Singh, R., editors, *Emerging Membrane Technology for Sustainable Water Treatment*, pages 15–52. Elsevier, Boston.

[24] Speed, D. (2016). 10 - environmental aspects of planarization processes. In Babu, S., editor, *Advances in Chemical Mechanical Planarization (CMP)*, pages 229–269. Woodhead Publishing.

[25] Stoffel, D., Rigo, E., Derlon, N., Staaks, C., Heijnen, M., Morgenroth, E., and Jacquin, C. (2022). Low maintenance gravity-driven membrane filtration using hollow fibers: Effect of reducing space for biofilm growth and control strategies on permeate flux. *Science of The Total Environment*, 811:152307.

[26] Ugarte, P., Ramo, A., Quílez, J., del Carmen Bordes, M., Mestre, S., Sánchez, E., Ángel Peña, J., and Menéndez, M. (2022). Low-cost ceramic membrane bioreactor: Effect of backwashing, relaxation and aeration on fouling. protozoa and bacteria removal. *Chemosphere*, 306:135587.

[27] Wu, B., Soon, G. Q. Y., and Chong, T. H. (2019). Recycling rainwater by submerged gravity-driven membrane (gdm) reactors: Effect of hydraulic retention time and periodic backwash. *Science of The Total Environment*, 654:10–18.

[28] Ziemba, C., Larivé, O., Reynaert, E., and Morgenroth, E. (2018). Chemical composition, nutrient-balancing and biological treatment of hand washing greywater. *Water Research*, 144:752–762.

Title of work:

Gravity-driven membrane filtration with hollow-fiber membranes operated in inside-out mode: distribution and characteristics of the biofilm inside and outside the fiber and feed-strategy effects on the performance

Thesis type and date:

Master Thesis, August 26, 2022

Supervision:

Prof. Dr. Urs von Gunten (EPFL)
Dr. Céline Jacquin (Eawag)

Student:

Name: Wei Yin
E-mail: wei.yin@epfl.ch
Legi-Nr.:
Semester:

Statement regarding plagiarism:

By signing this statement, I affirm that I have read and signed the Declaration of Originality, independently produced this paper, and adhered to the general practice of source citation in this subject-area.

Declaration of Originality:

http://www.ethz.ch/faculty/exams/plagiarism/confirmation_en.pdf

Zurich, 26. 8. 2022: _____